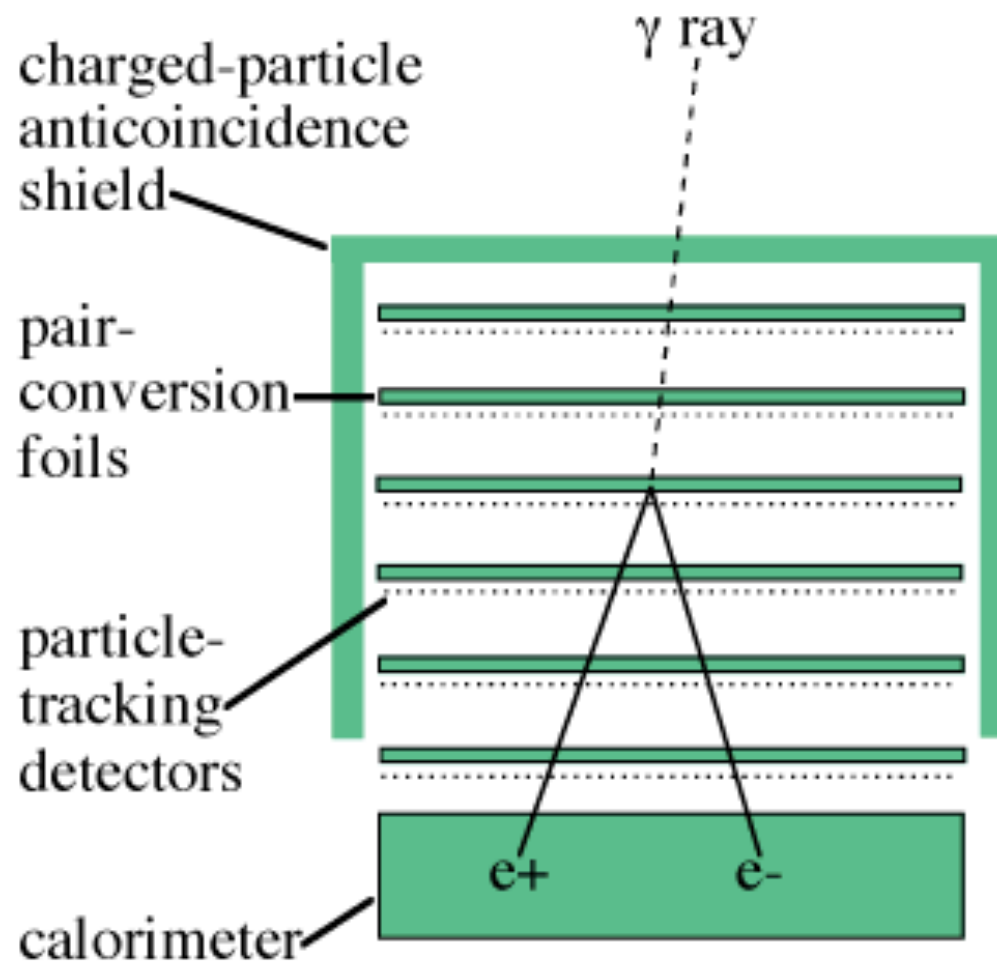


Astrofisica Nucleare e Subnucleare
GeV Astrophysics

Detector Project



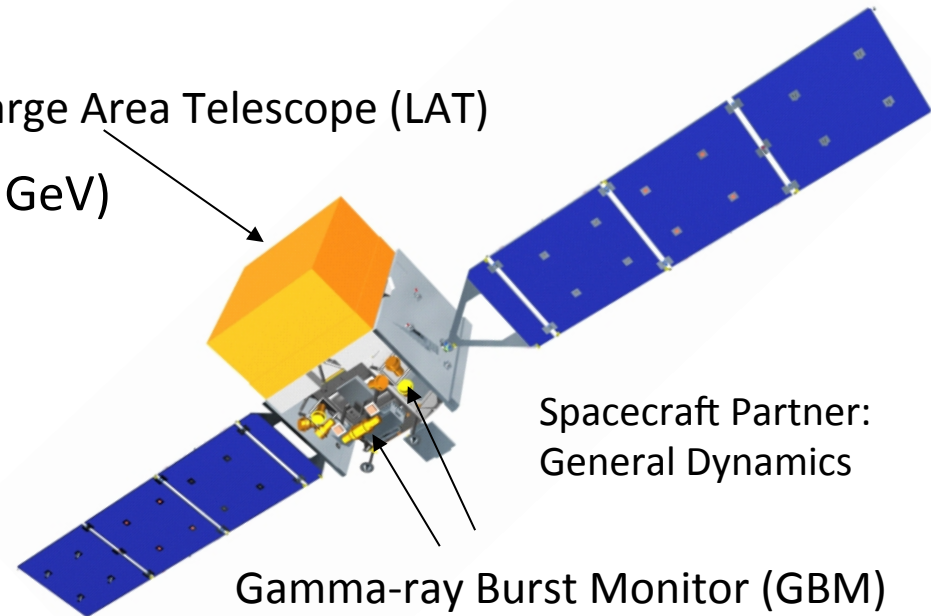
Fermi LAT

Key Features

- Two instruments:

- LAT:
 - high energy (20 MeV – >300 GeV)
- GBM:
 - low energy (8 keV – 40 MeV)

Large Area Telescope (LAT)



Spacecraft Partner:
General Dynamics

Gamma-ray Burst Monitor (GBM)

- Huge field of view

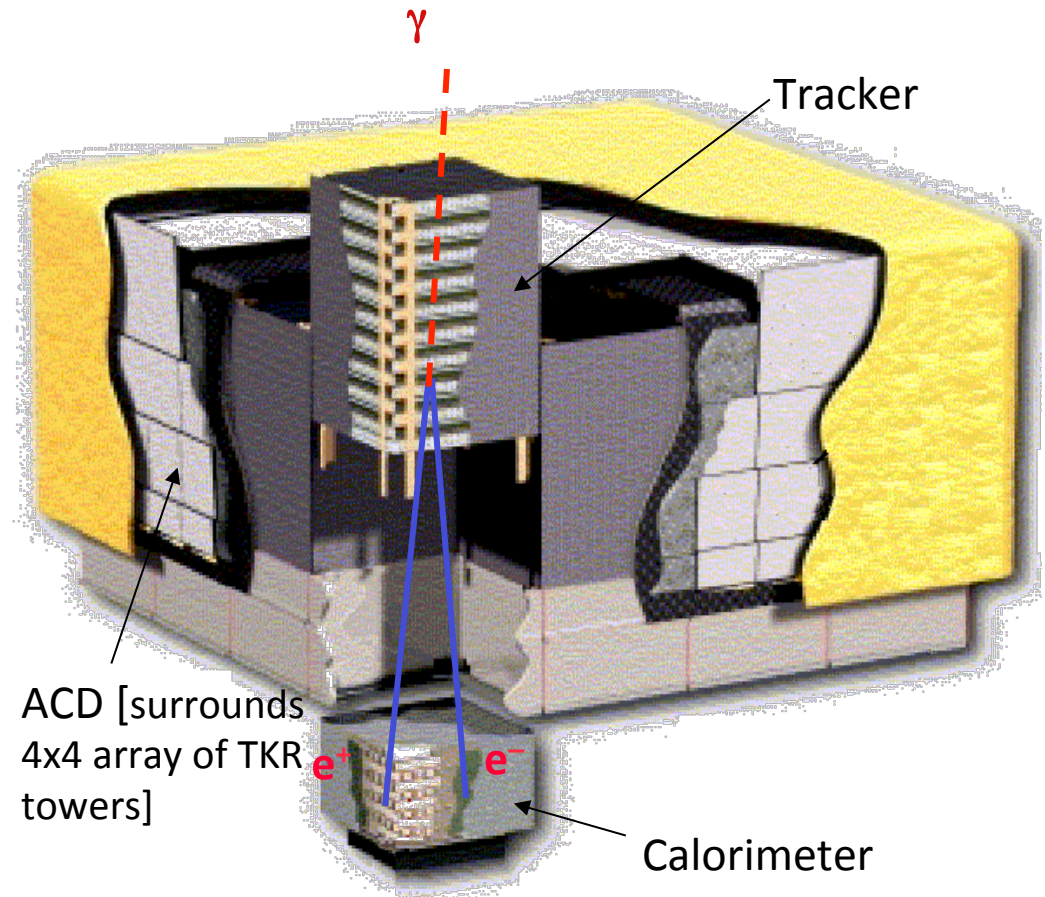
- LAT: 20% of the sky at any instant; in sky survey mode, expose all parts of sky for ~30 minutes every 3 hours. GBM: whole unocculted sky at any time.

- Huge energy range, including largely unexplored band 10 GeV - 100 GeV

- Large leap in all key capabilities. Great discovery potential.

Overview of LAT

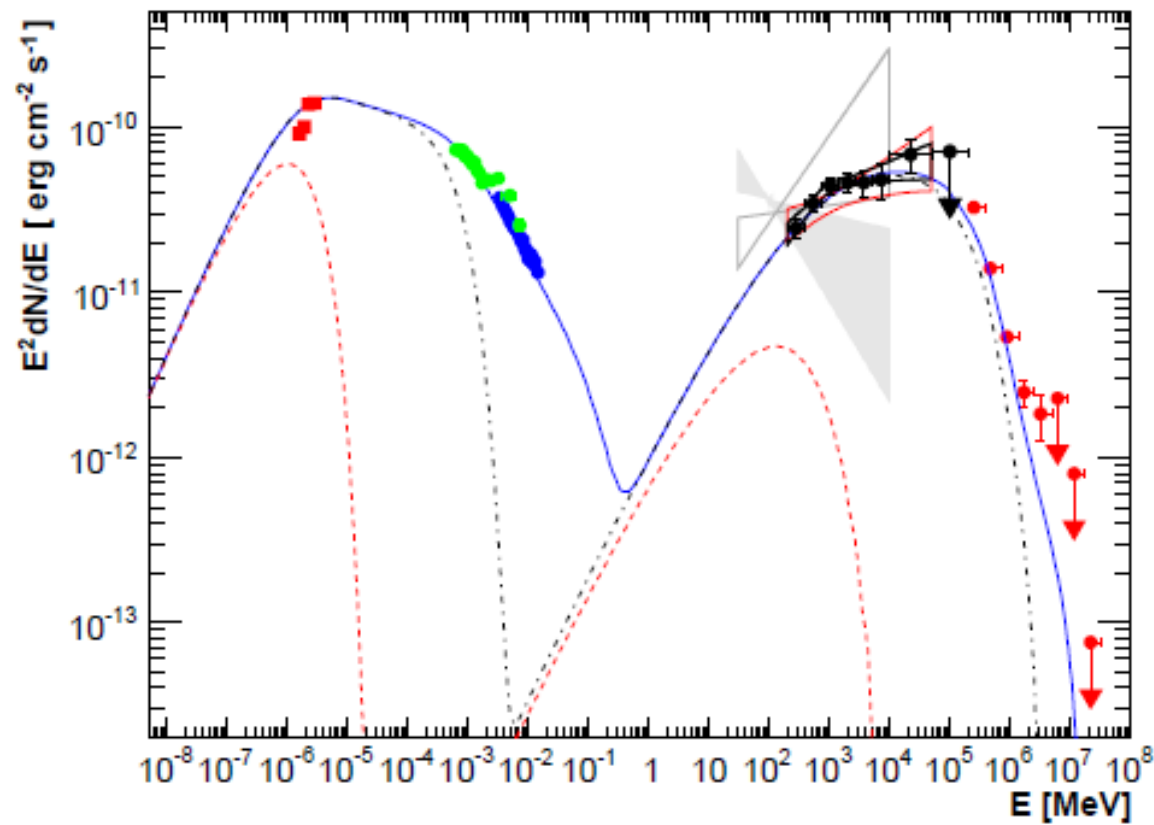
- Precision Si-strip Tracker (TKR) 18 XY tracking planes. Single-sided silicon strip detectors (228 μm pitch) Measure the photon direction; gamma ID.
- Hodoscopic CsI Calorimeter(CAL) Array of 1536 CsI(Tl) crystals in 8 layers. Measure the photon energy; image the shower.
- Segmented Anticoincidence Detector (ACD) 89 plastic scintillator tiles. Reject background of charged cosmic rays; segmentation removes self-veto effects at high energy.
- Electronics System Includes flexible, robust hardware trigger and software filters.



Systems work together to identify and measure the flux of cosmic gamma rays with energy 20 MeV - >300 GeV.

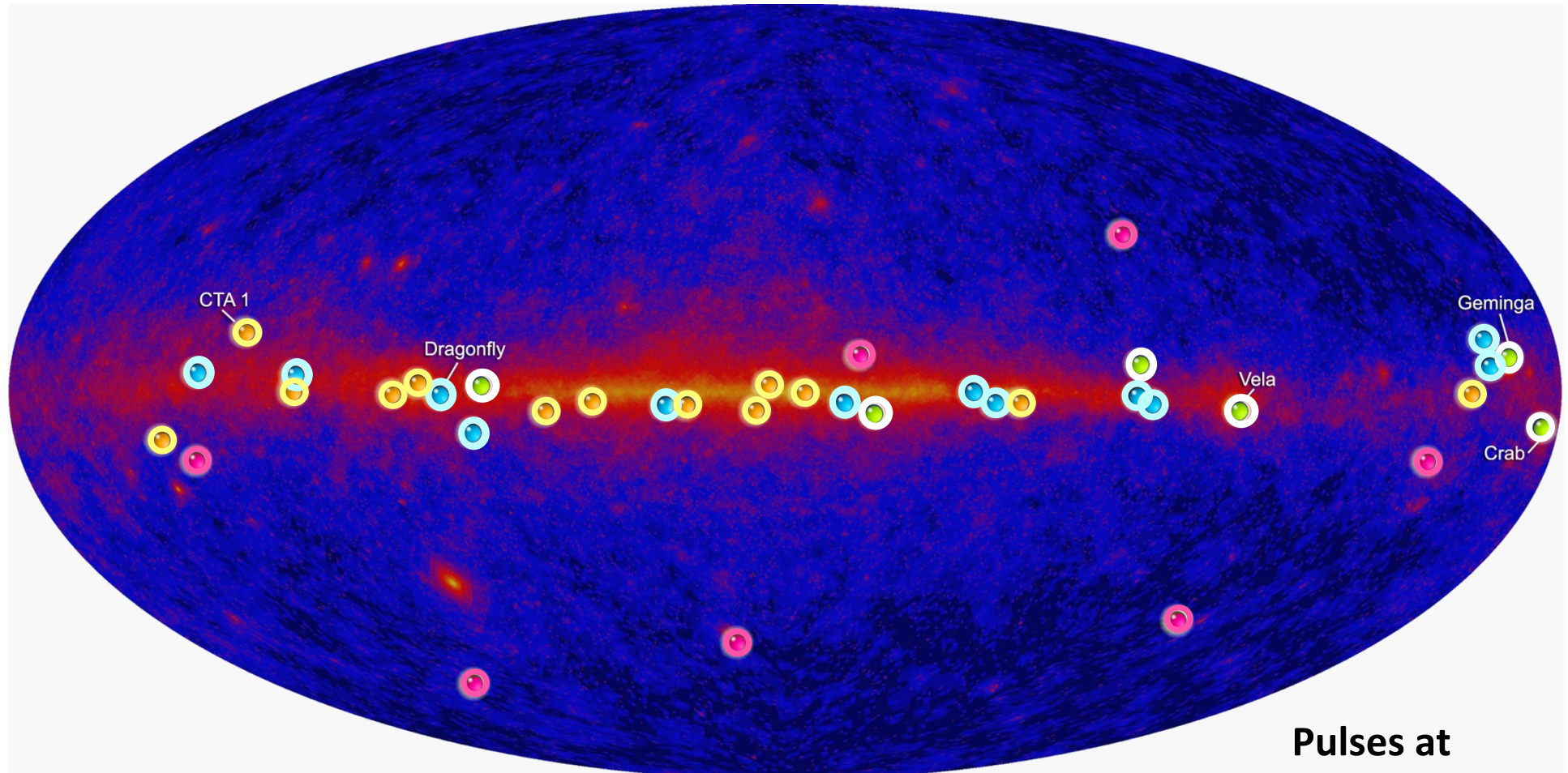
Challenge # 1 – AGN

Joint campaign on PKS 2155 with HESS



Aharonian et al. 2009

Challenge # 2 – Pulsars Blind Search

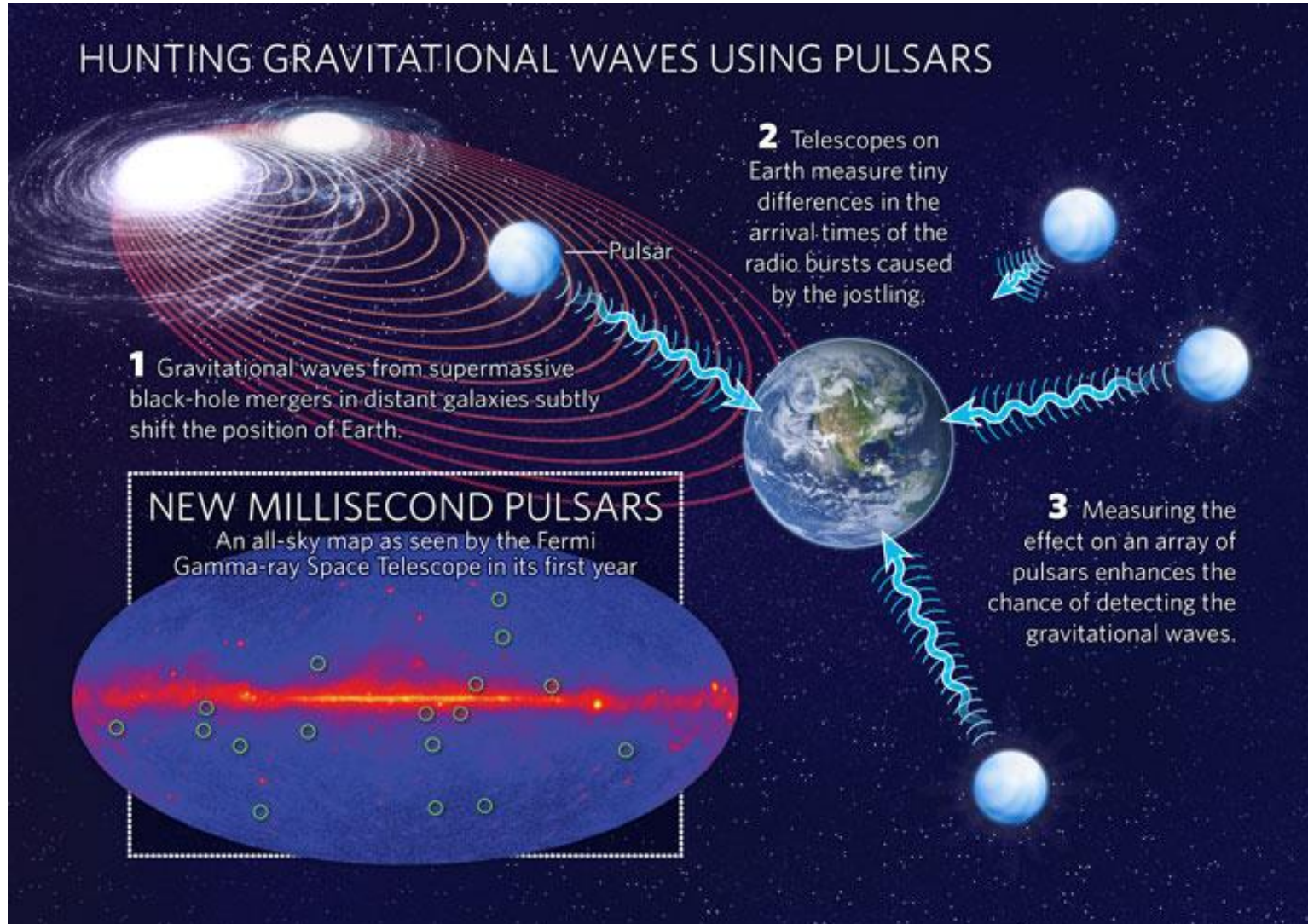


Fermi Pulsar Detections

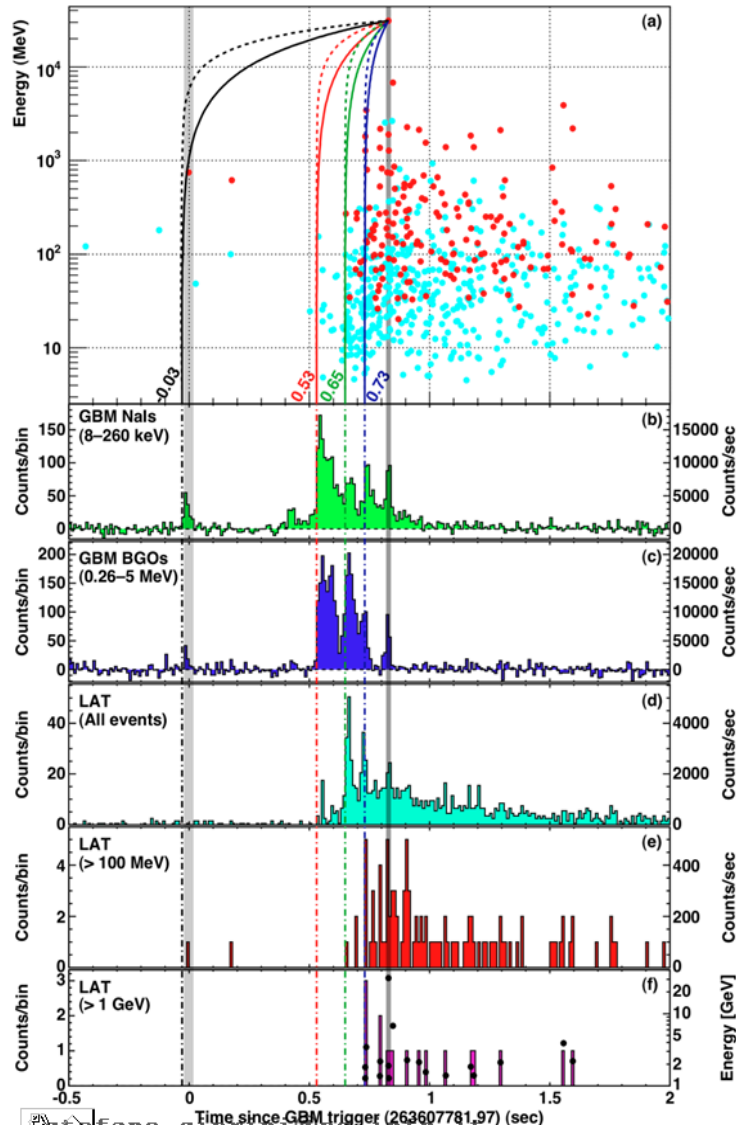
Abdo et al..2010

- New pulsars discovered in a blind search
 - Millisecond radio pulsars
 - Young radio pulsars
 - Confirmed pulsars seen by Compton Observatory EGRET instrument
- Pulses at 1/10th true rate**

New MSP and GW detection



Challenge # 3 – GRB



- ❑ This GRB is a perfect case for studying Lorentz Invariance Violation
 - ❑ $z = 0.9$ (5.381 Gyr)
 - ❑ Emission of 31 GeV photon after 859 ms since the trigger
- ❑ Only conservative assumption!
 - ❑ the HE photon is not emitted *before* the LE photons, at different events.

Table 2 | Limits on Lorentz Invariance Violation

#	$t_{\text{start}} - T_0$ (ms)	Limit on $ \Delta t $ (ms)	Reasoning for choice of t_{start} or limit on Δt or $ \Delta t/\Delta E $	E_1^\dagger (MeV)	Valid for s_n^*	Lower limit on $M_{\text{QG},1}/M_{\text{Planck}}$
(a)*	-30	< 859	start of any < 1 MeV emission	0.1	1	> 1.19
(b)*	530	< 299	start of main < 1 MeV emission	0.1	1	> 3.42
(c)*	648	< 181	start of main > 0.1 GeV emission	100	1	> 5.63
(d)*	730	< 99	start of > 1 GeV emission	1000	1	> 10.0
(e)*	—	< 10	association with < 1 MeV spike	0.1	± 1	> 102
(f)*	—	< 19	If 0.75 GeV ‡ γ -ray from 1 st spike	0.1	-1	> 1.33
(g)*	$ \Delta t/\Delta E < 30 \text{ ms/GeV}$	—	lag analysis of > 1 GeV spikes	—	± 1	> 1.22

[nature](#) > [letters](#) > article

[Published: 01 October 1998](#)

Tests of quantum gravity from observations of γ -ray bursts

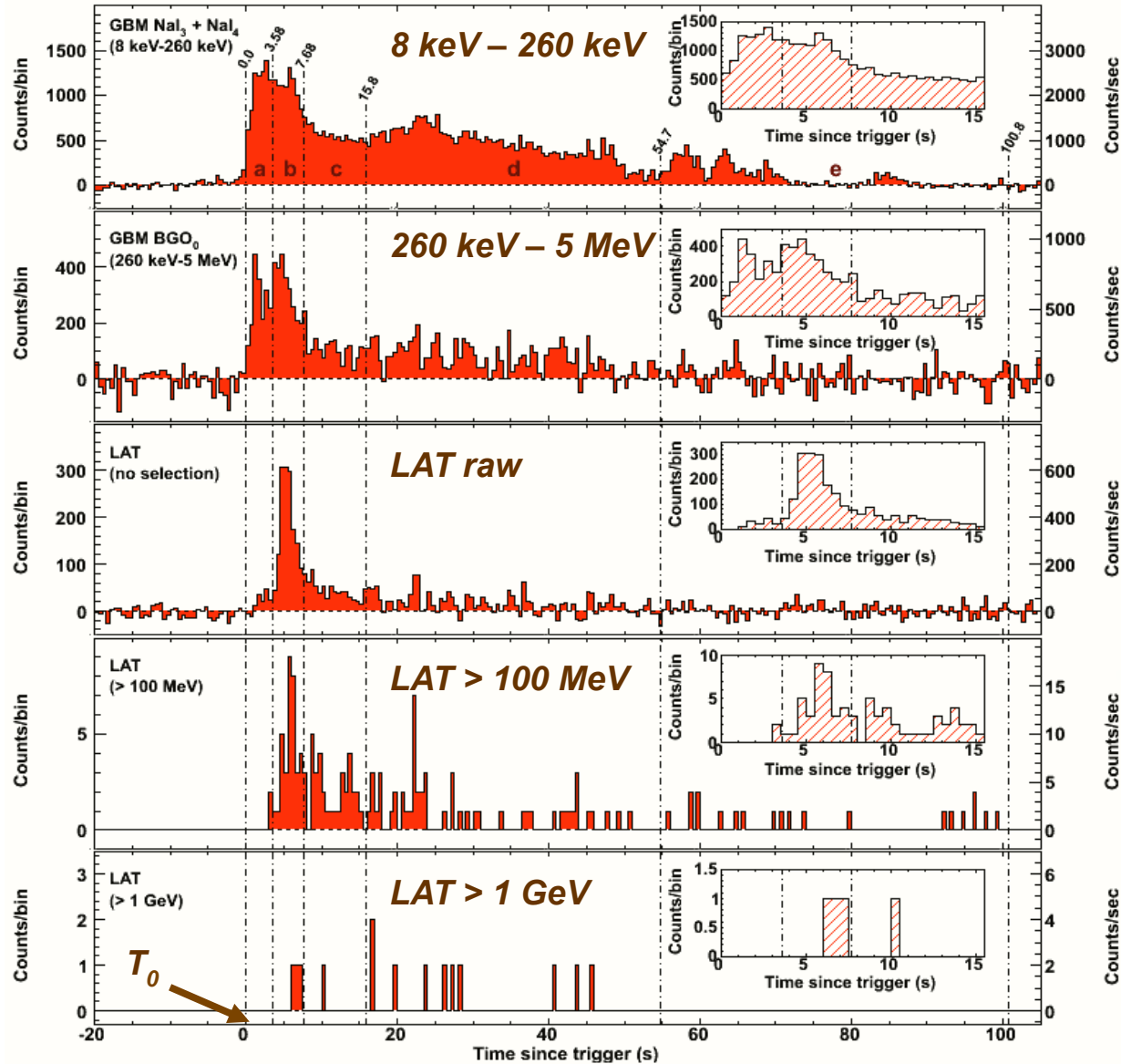
[G. Amelino-Camelia](#), [John Ellis](#), [N. E. Mavromatos](#), [D. V. Nanopoulos](#) & [Subir Sarkar](#)

[Nature](#) **395**, 525 (1998) | [Cite this article](#)

The recent confirmation that at least some γ -ray bursts originate at cosmological distances¹⁻⁴ suggests that the radiation from them could be used to probe some of the fundamental laws of physics. Here we show that γ -ray bursts will be sensitive to an energy dispersion predicted by some approaches to quantum gravity. Many of the bursts have structure on relatively rapid timescales⁵, which means that in principle it is possible to look for energy-dependent dispersion of the radiation, manifested in the arrival times of the photons, if several different energy bands are observed simultaneously. A simple estimate indicates that, because of their high energies and distant origin, observations of these bursts should be sensitive to a dispersion scale that is comparable to the Planck energy scale ($\sim 10^{19}$ GeV), which is sufficient to test theories of quantum gravity. Such observations are already possible using existing γ -ray burst detectors.

$$v = \frac{\partial E}{\partial p} \approx c \left(1 - \xi \frac{E}{E_{\text{QG}}} \right) \quad \Delta t \approx \xi \frac{E}{E_{\text{QG}}} \frac{L}{c}$$

GRB080916C - Multiple detector light curve



First 3 light curves are background subtracted

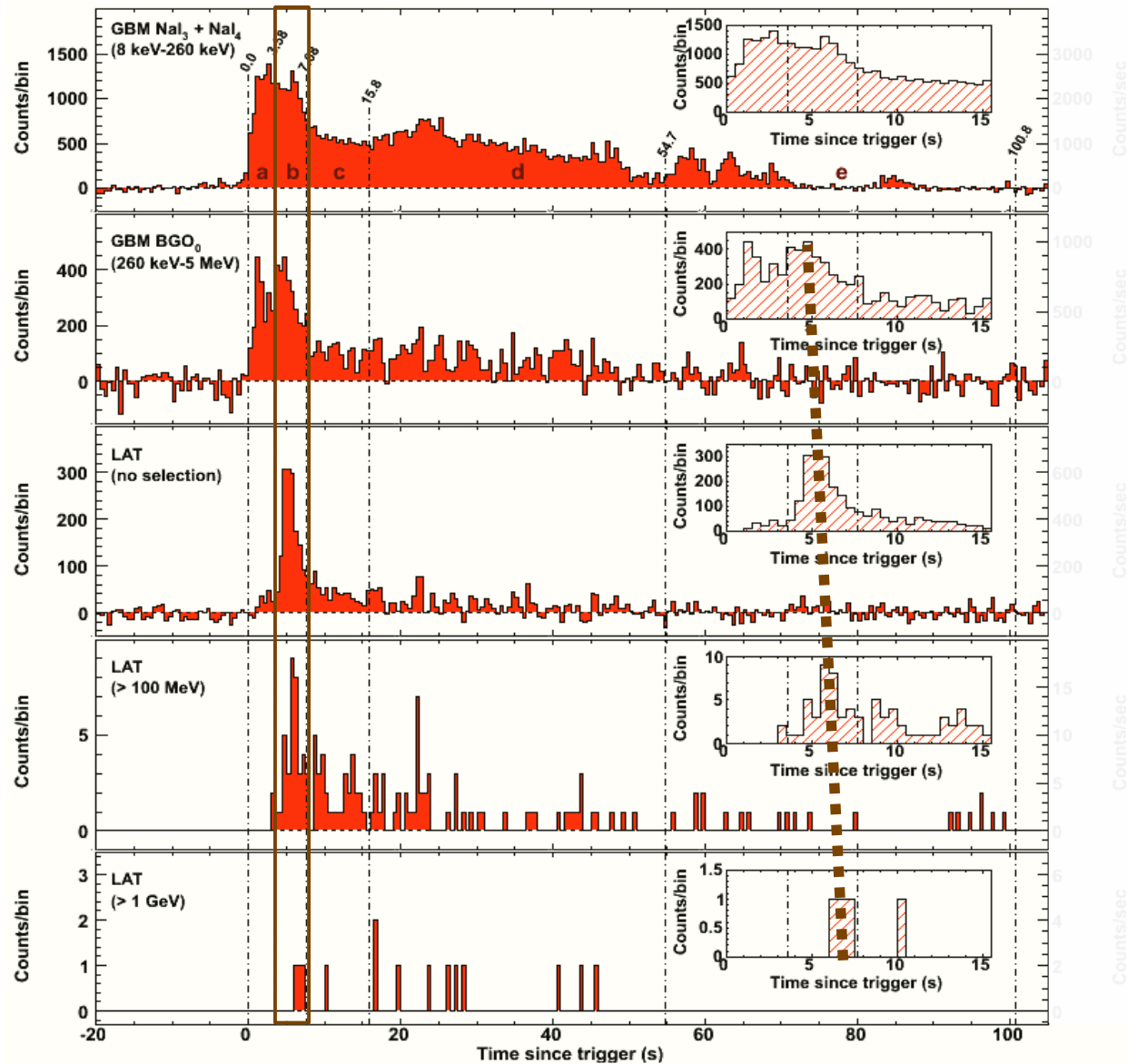
The LAT can be used as a **counter** to maximize the rate and to study time structures above tens of MeV

- The first low-energy peak is not observed at LAT energies

Spectroscopy needs LAT event selection (>100 MeV)

- 14 events above 1 GeV

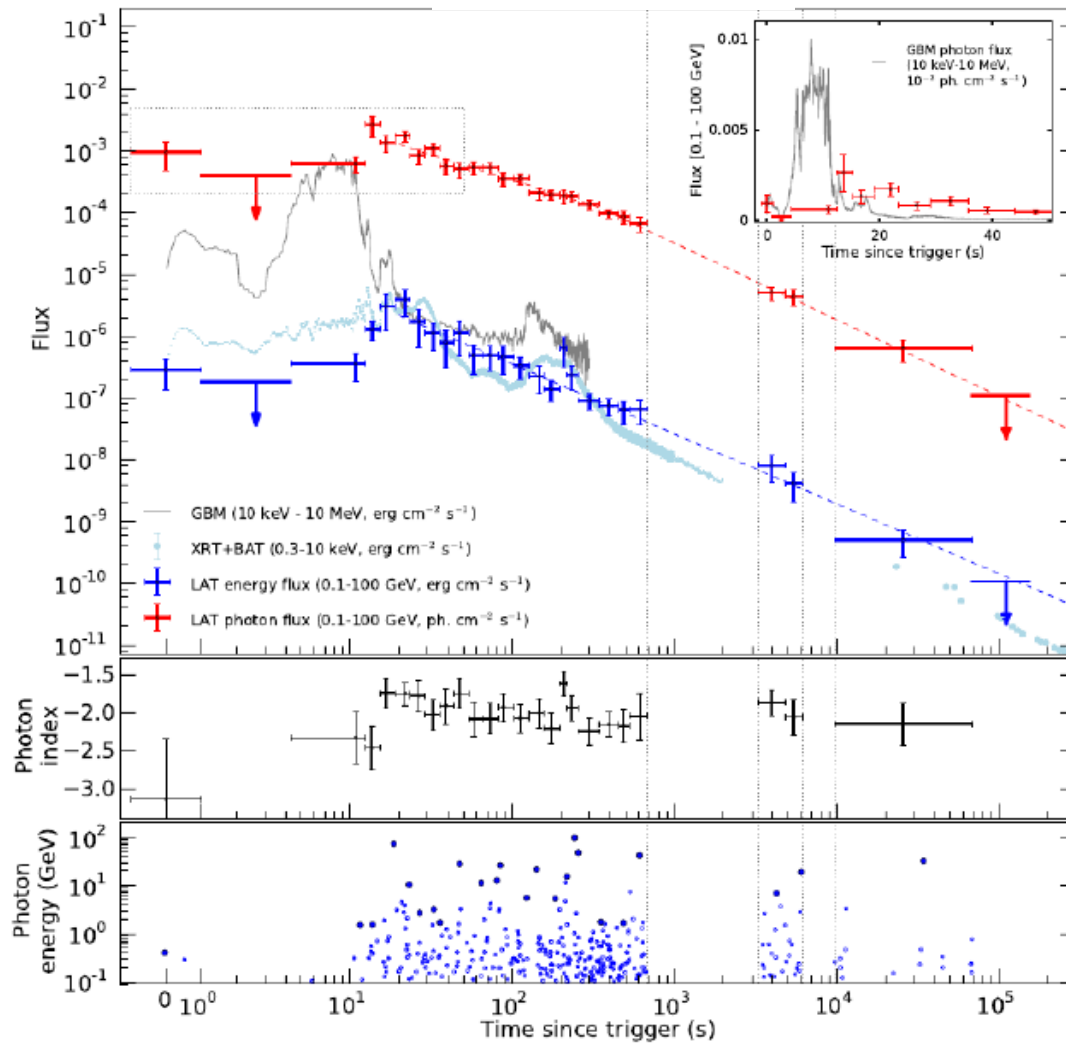
Multiple detector light curve



The bulk of the emission of the 2nd peak is moving toward later times as the energy increases

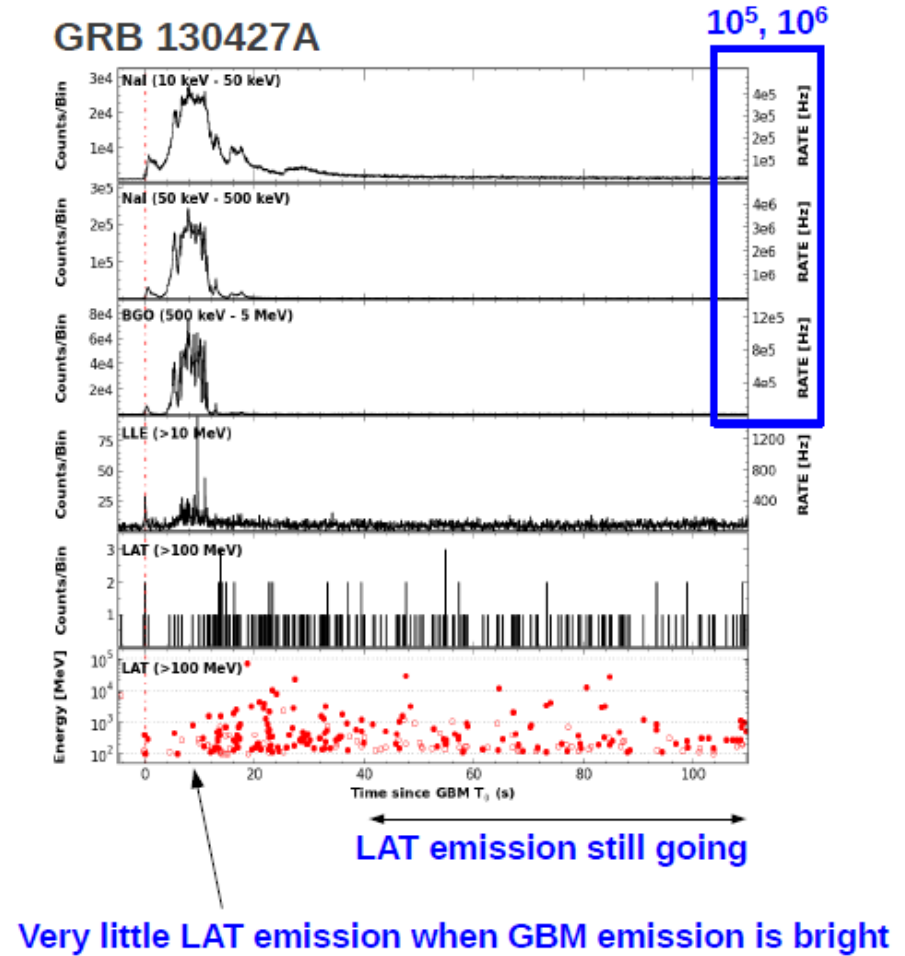
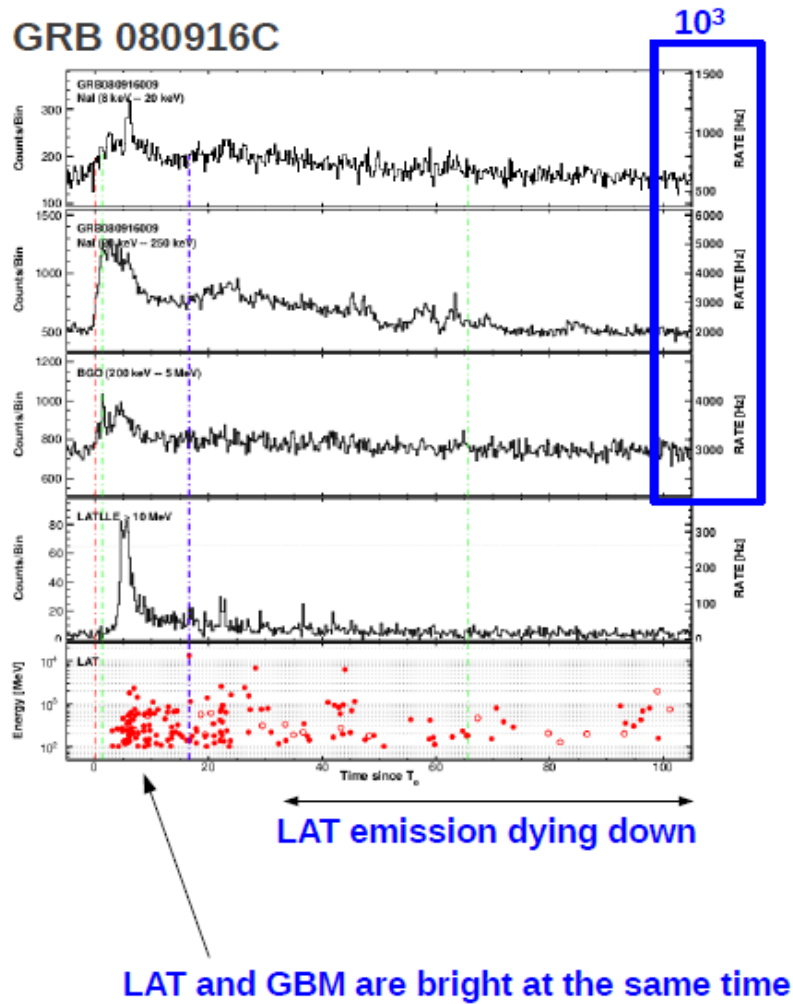
Clear signature of spectral evolution

GRB 130427A



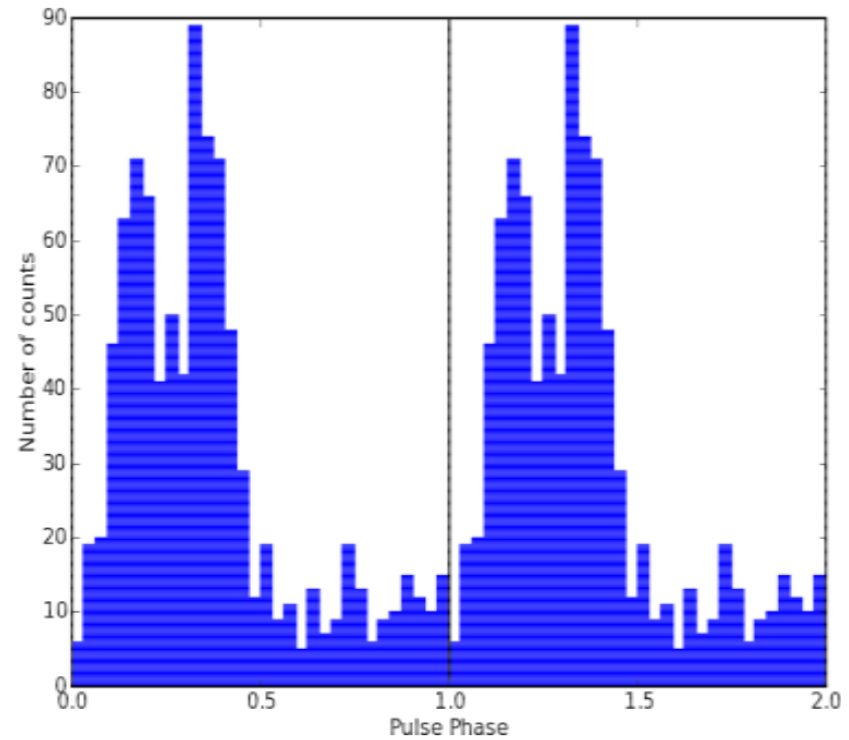
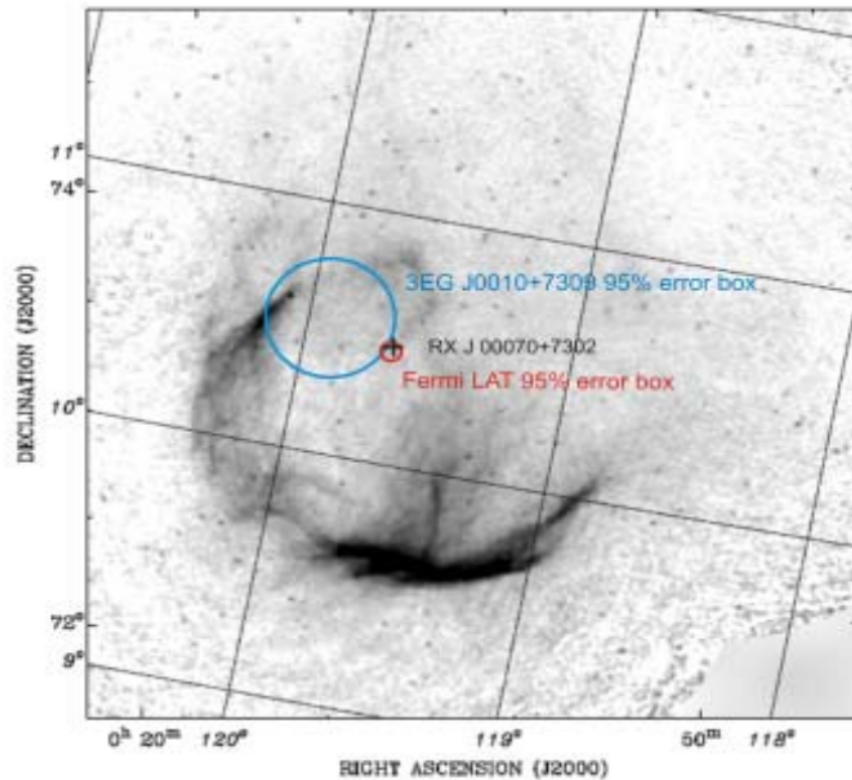
(Ackermann et al.,
Science, Vol. 343 no. 6166
pp. 42-47)

GRB 130427A



Challenge # 4 – Unidentified

CTA 1 Discovery

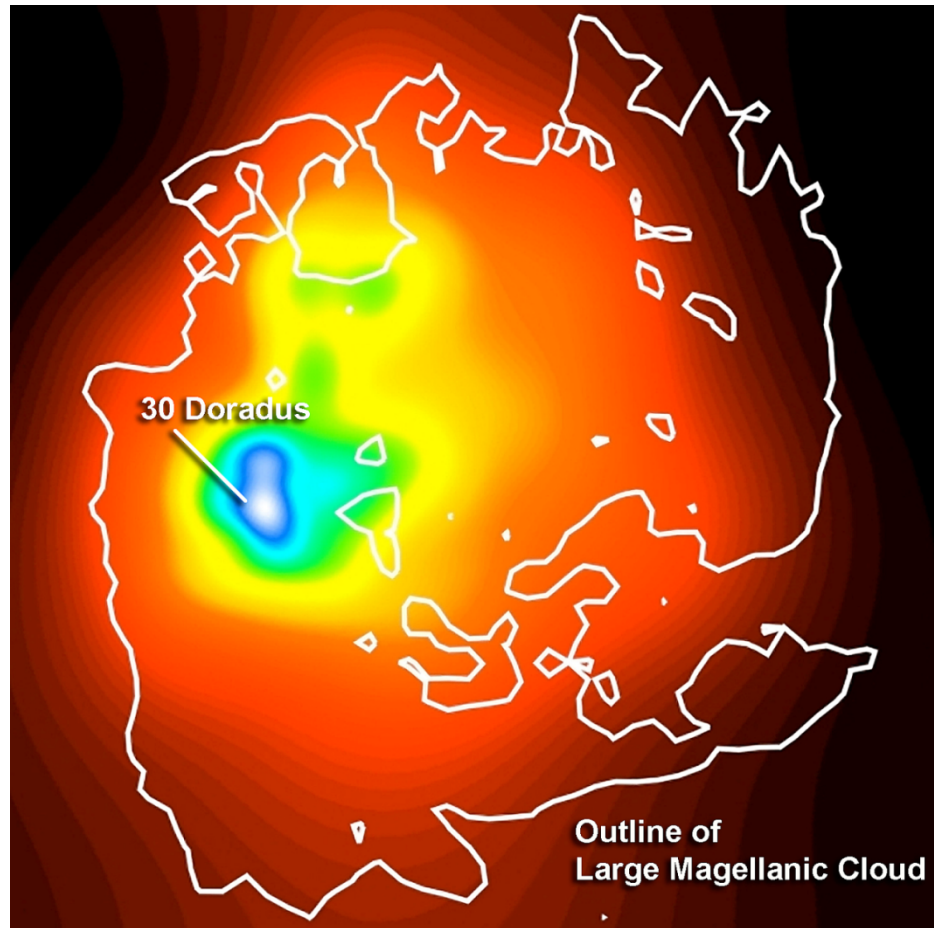


Abdo et al. 2008

Challenge # 4

Location of Gamma-ray emission

Observations of the Large Magellanic Cloud with *Fermi*

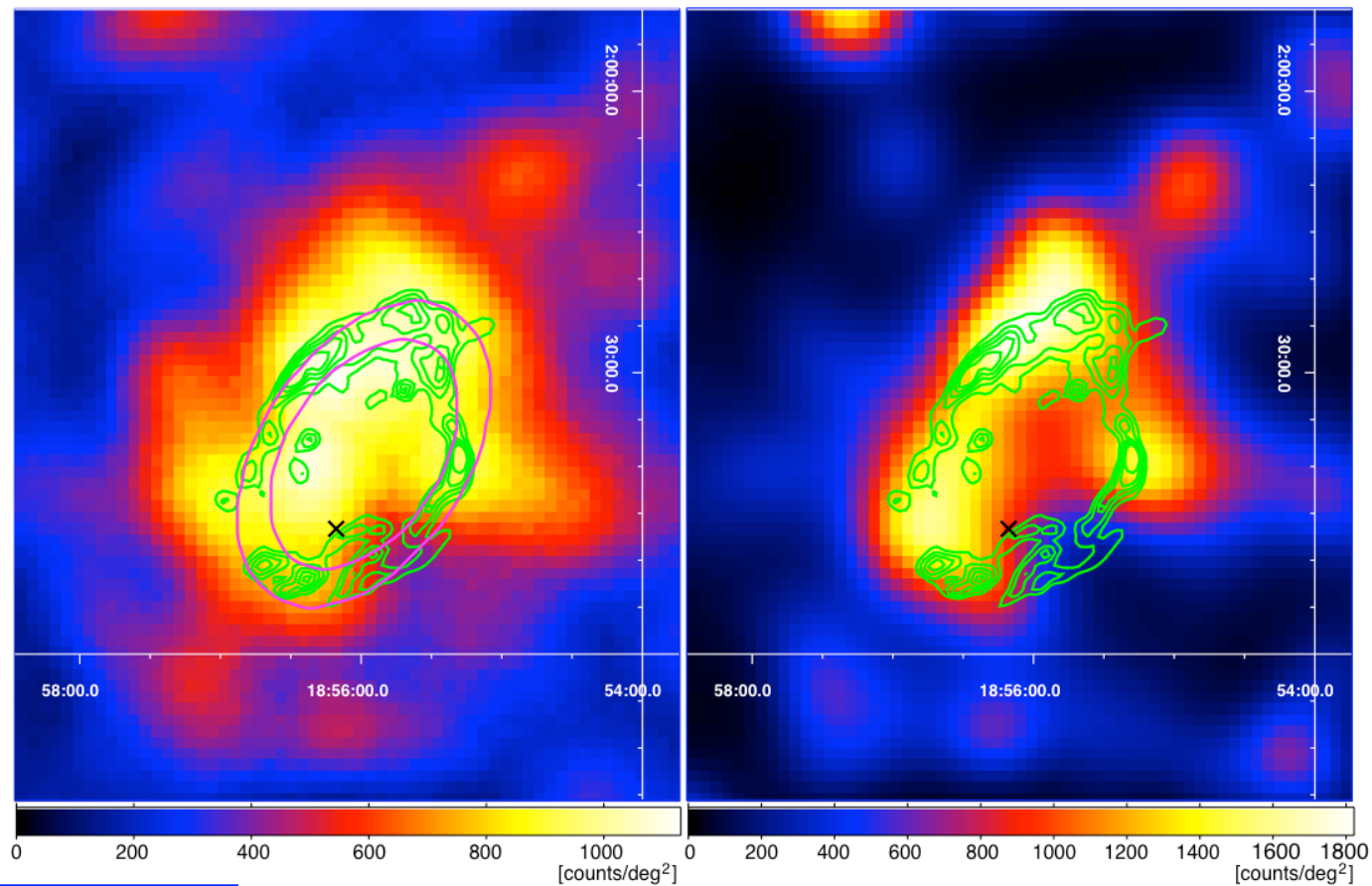


Abdo, A. A. et al. 2010

Challenge # 4

Location of Gamma-ray emission

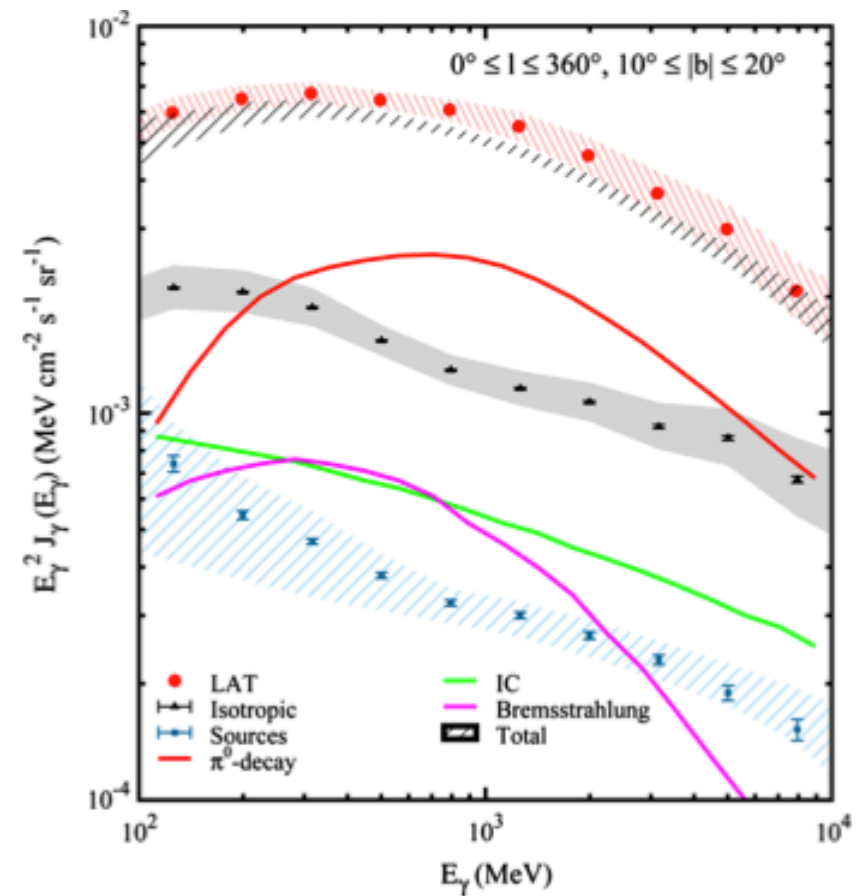
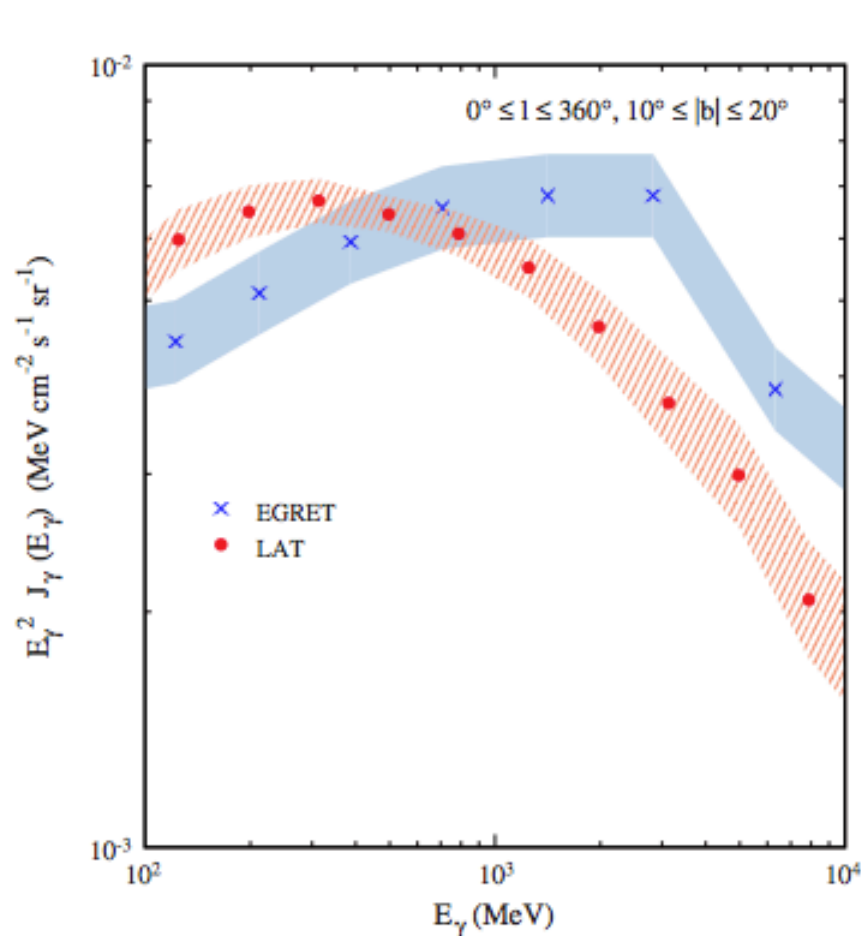
Gamma-Ray Emission from the Shell of Supernova Remnant W44 Revealed by the Fermi LAT



Abdo, A. A. et al. 2010

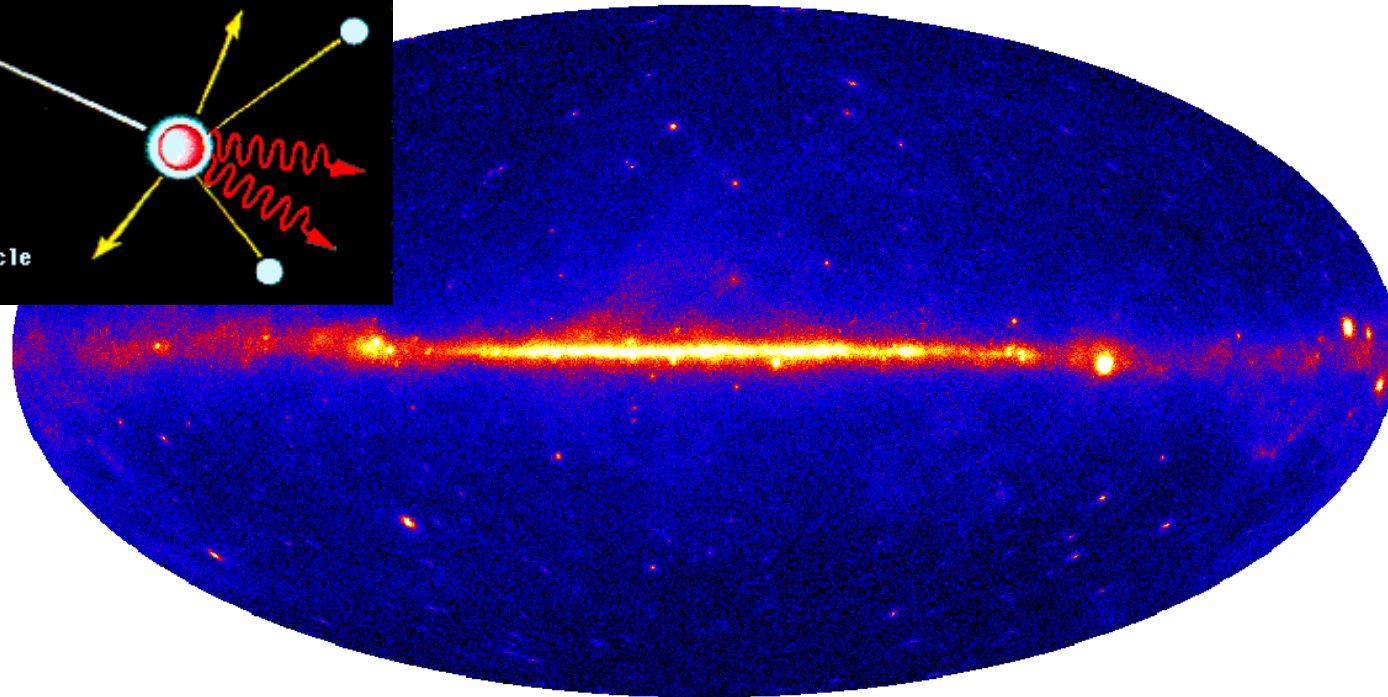
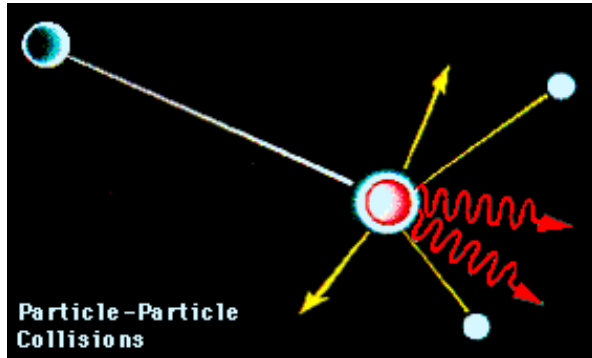
Challenge # 5 – Spectral Resolution

Fermi Large Area Telescope Measurements of the Diffuse Gamma-Ray Emission at Intermediate Galactic Latitudes



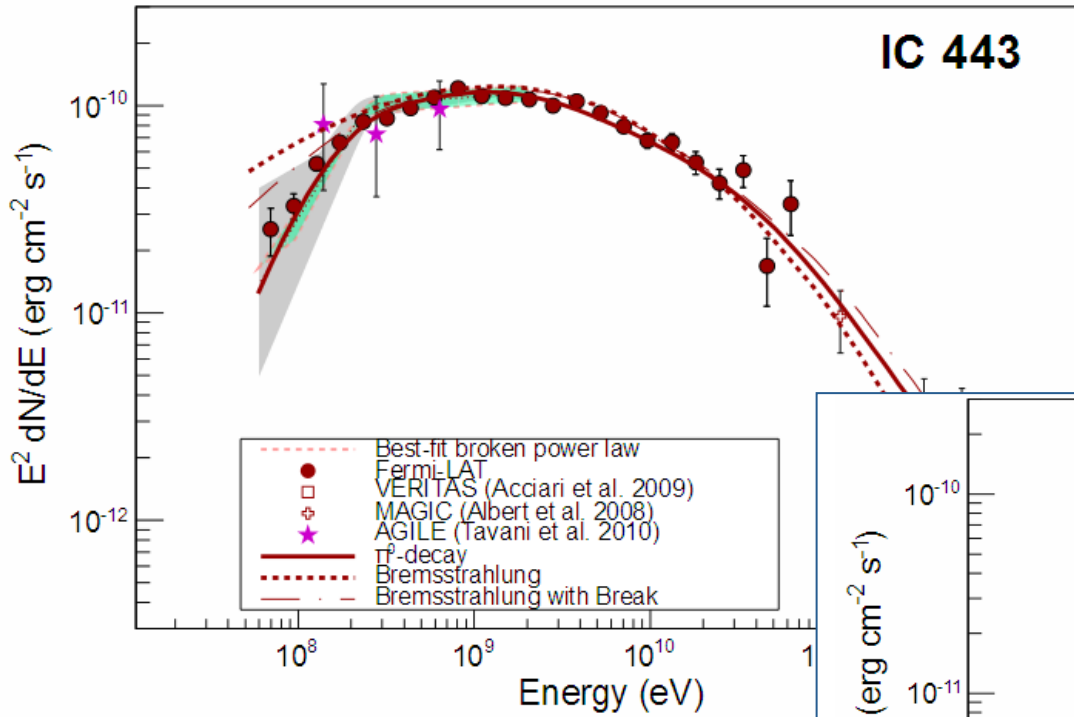
Abdo, A. A. et al. 2009

Cosmic Rays – Gamma-rays connection

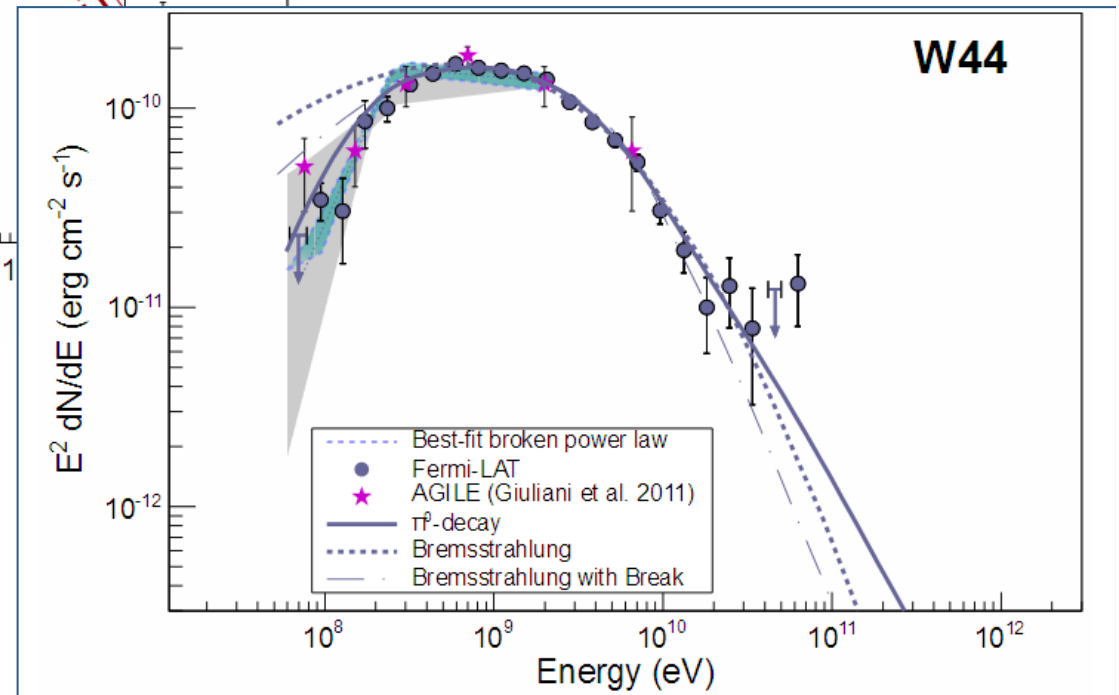


- Galactic gamma rays trace cosmic-ray proton interactions (cosmic-ray acceleration sites & propagation)
- Observations of nearby galaxies provide an outside view
- Primary targets: galactic plane, starburst galaxies, LMC, SNR
- Direct CR observations

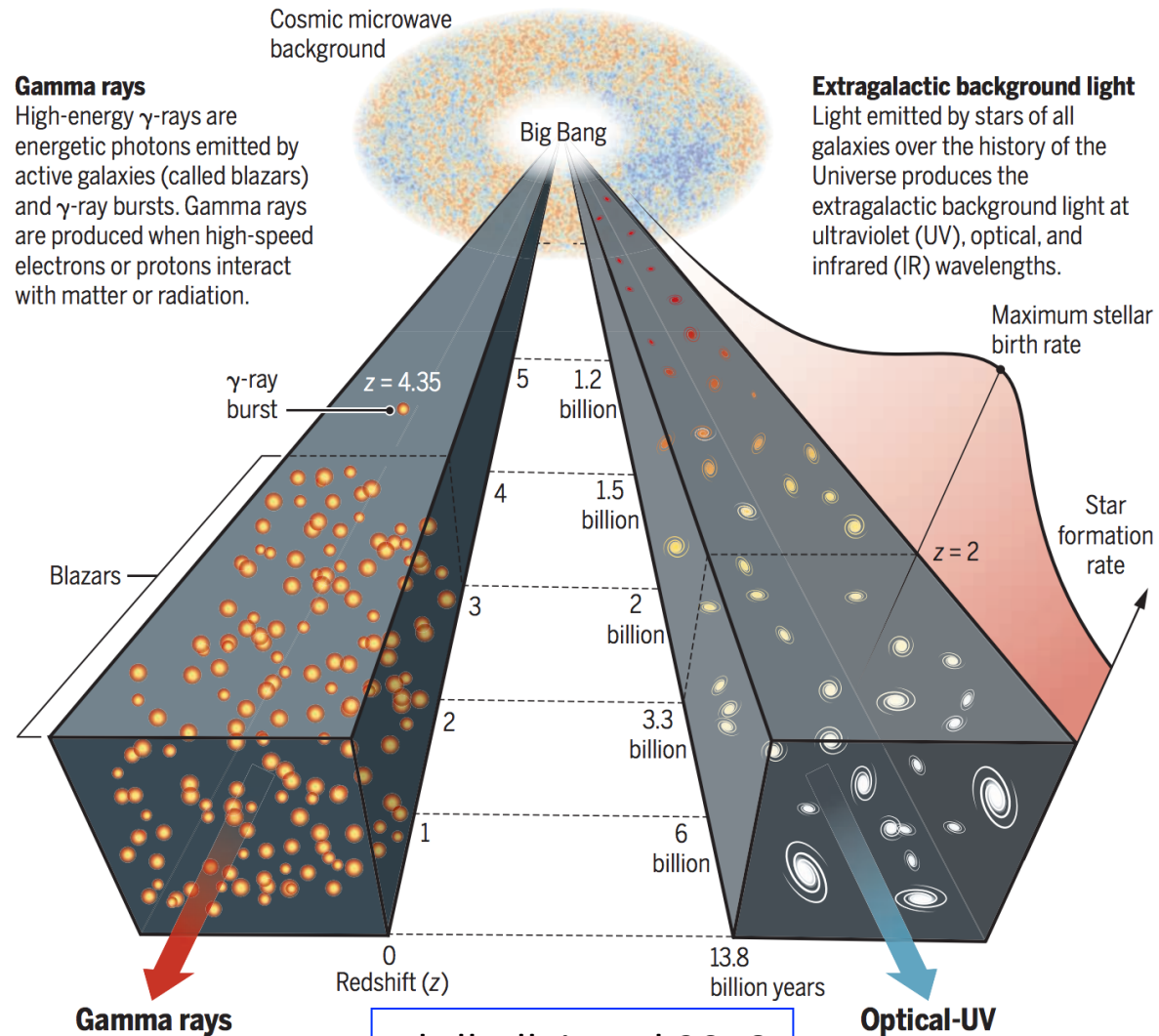
Supernova Remnants



Ackermann et al. 2013

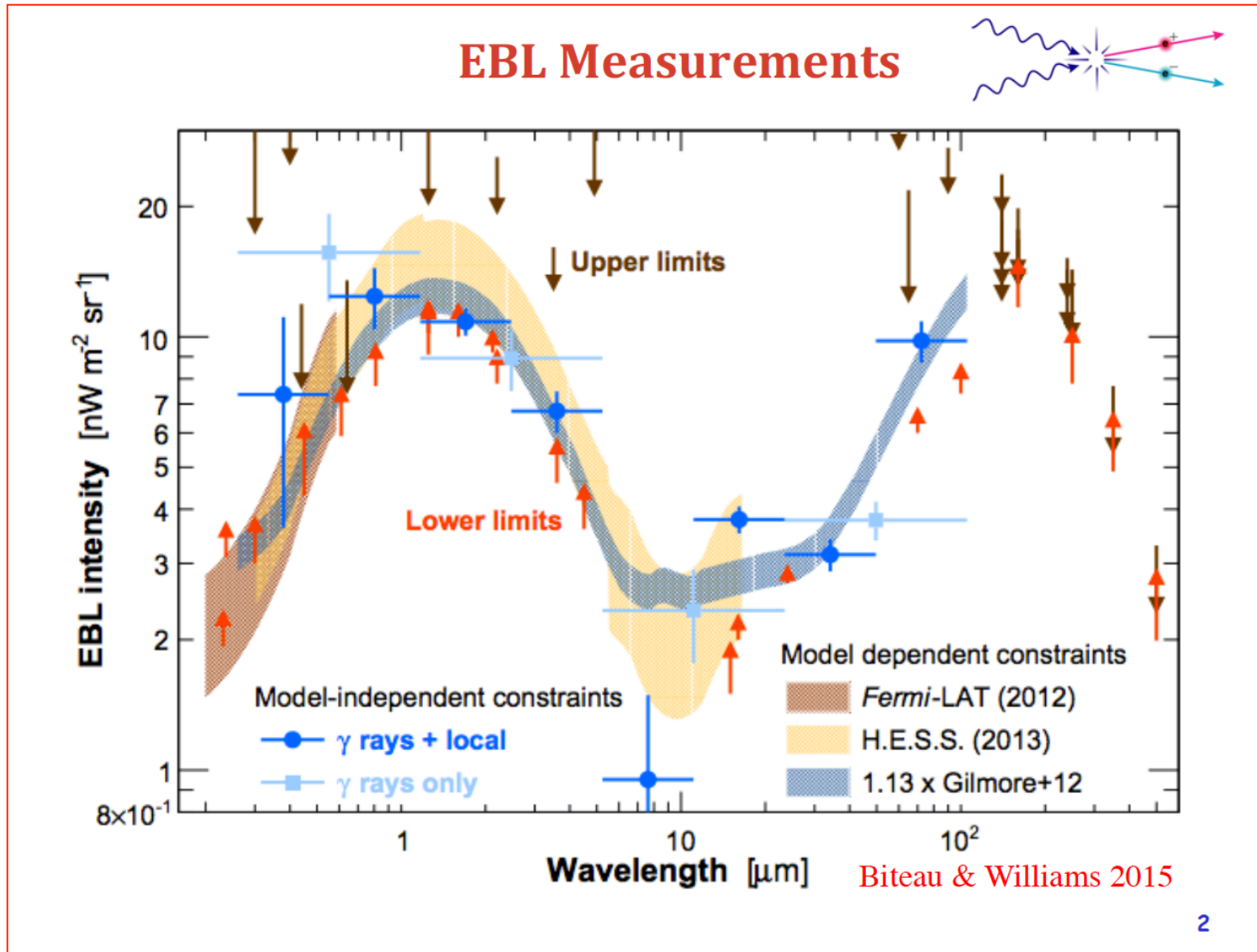


The EBL



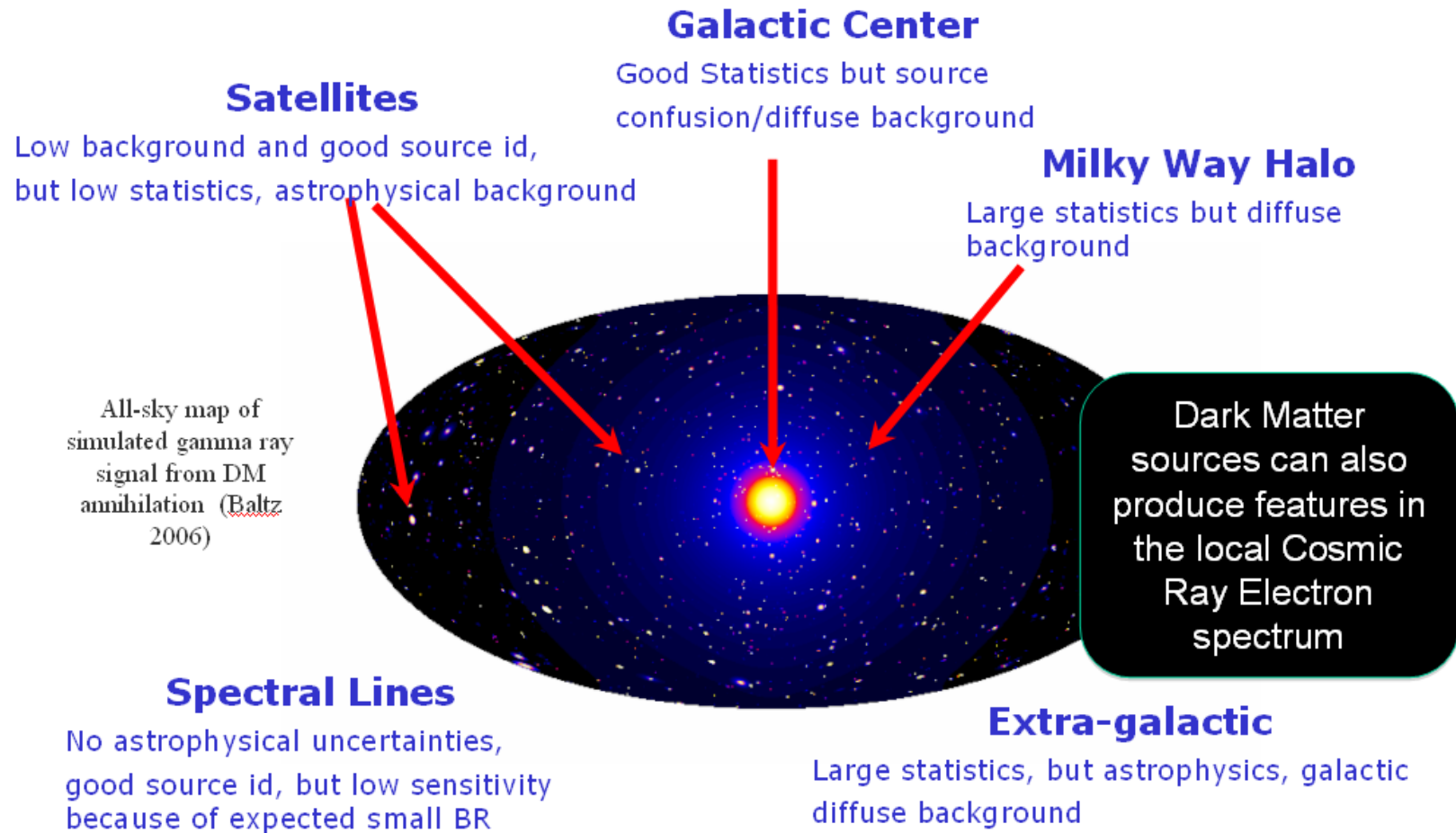
Abdollahi et al 2018

The Extragalactic Background Light

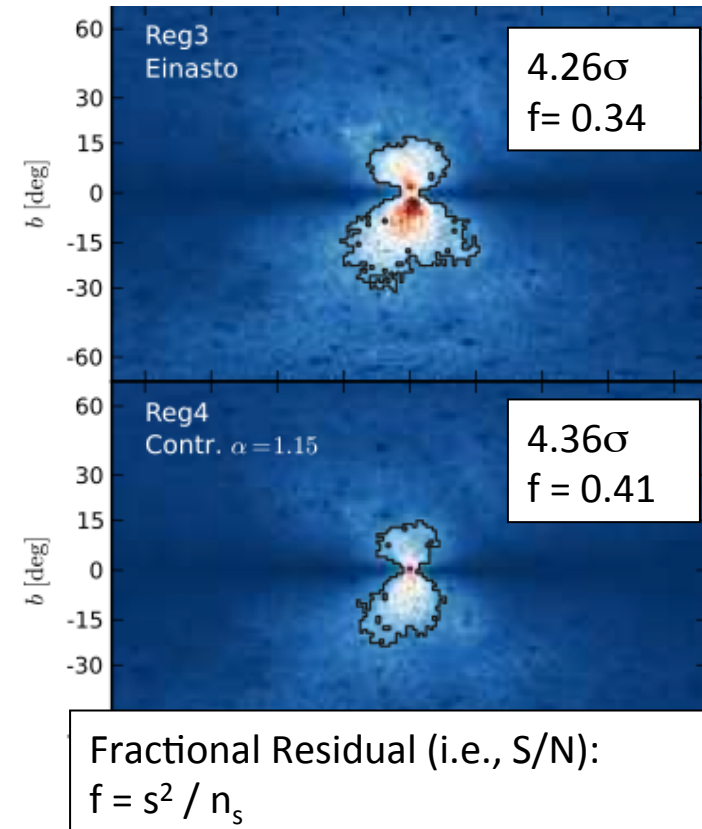
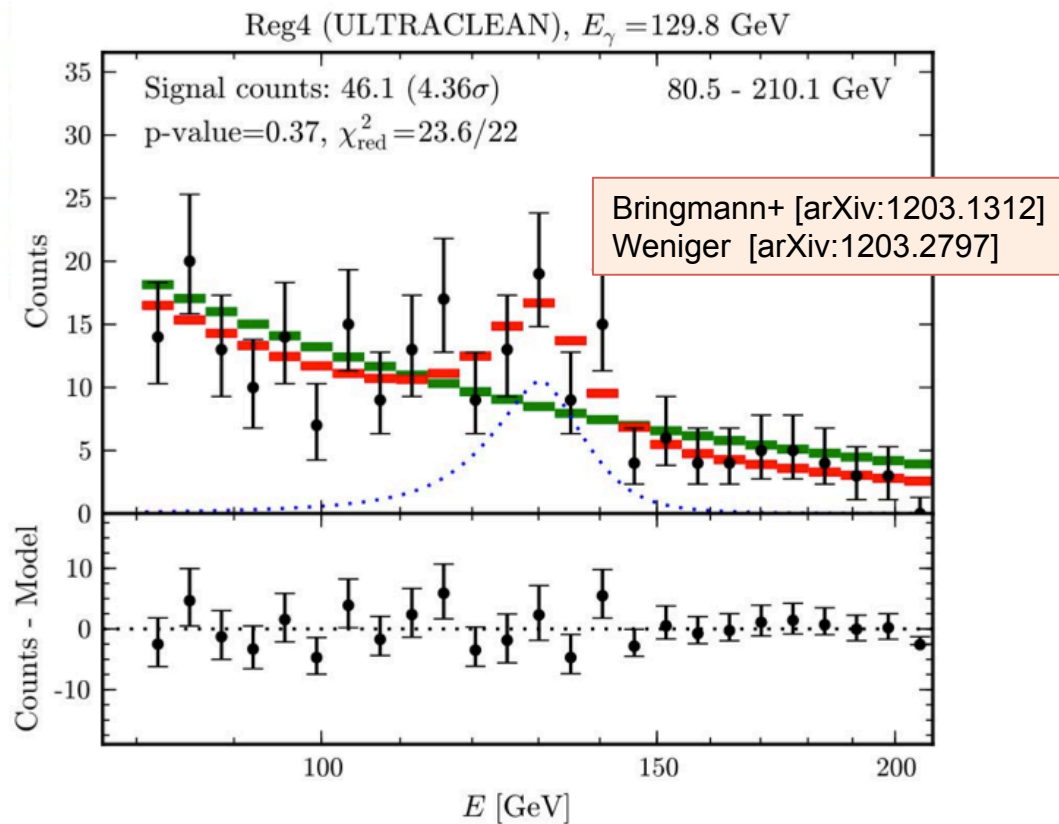


Dark Matter Searches

Gamma-ray indirect emission



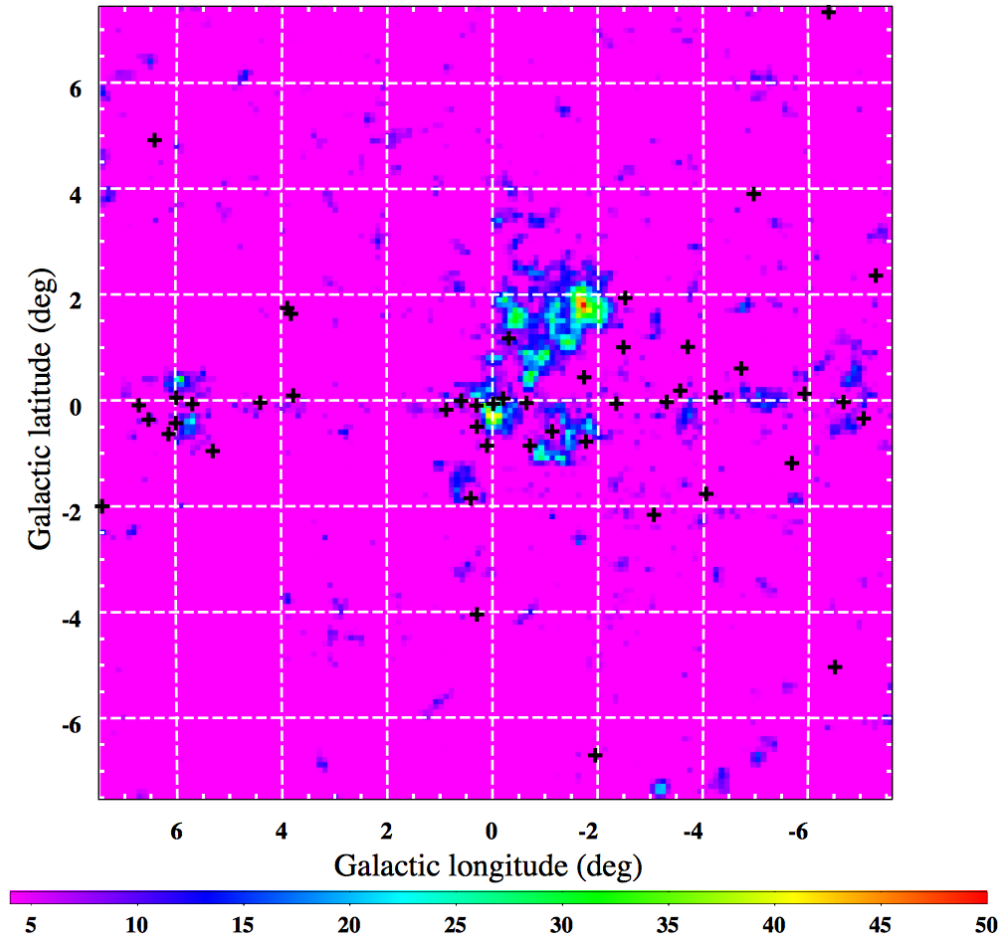
Narrow Spectral Feature at 130 GeV



Bringmann et al. and Weniger showed evidence for a narrow spectral feature near 130 GeV near the Galactic center (GC) in the LAT data.

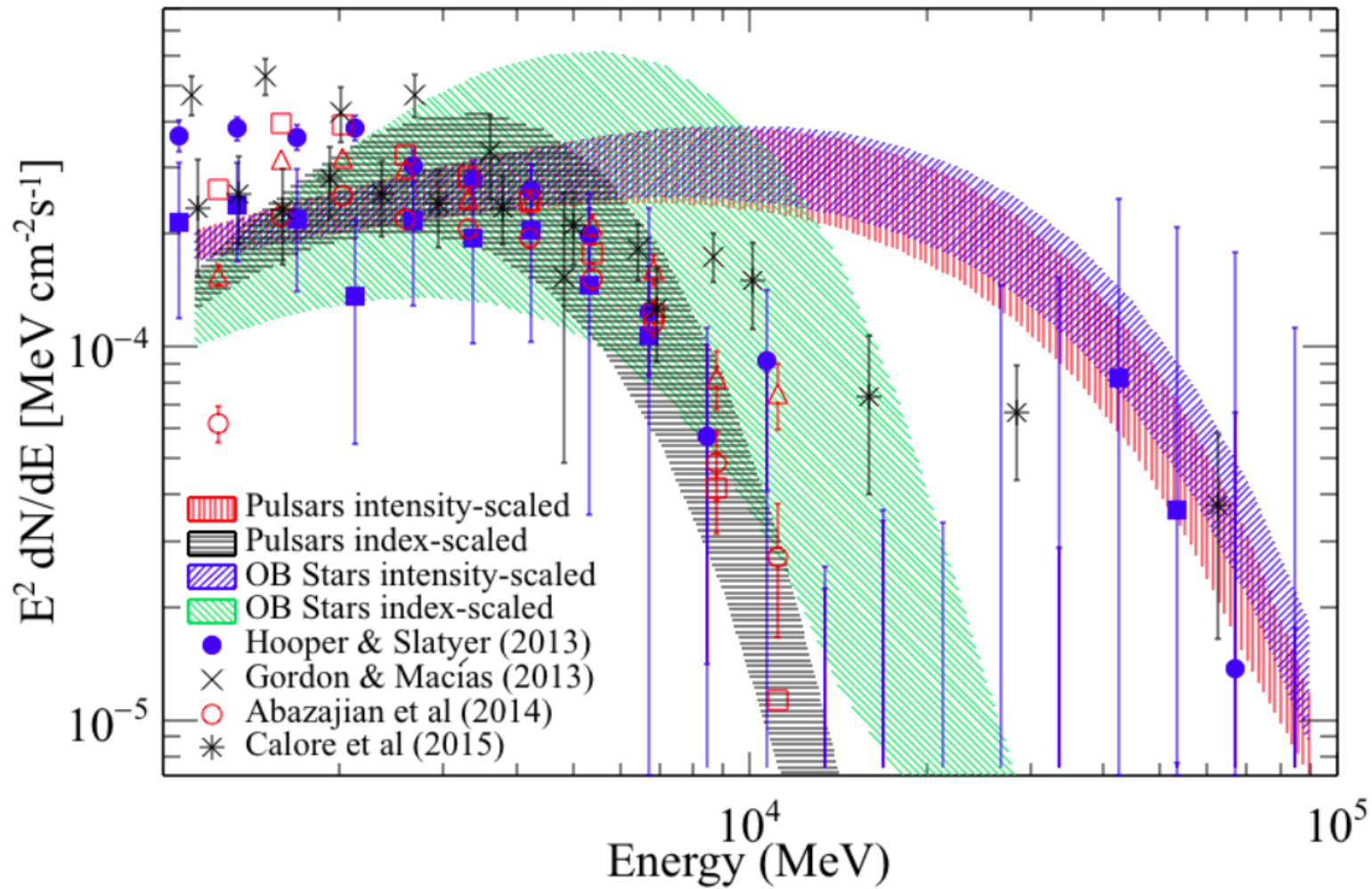
- Signal is particularly strong in 2 out of 5 test regions, shown above.
- Over 4σ local significance with $S/N > 30\%$, up to $\sim 60\%$ in optimized ROI.
- Some indication of double line (111 & 130 GeV).

Dark Matter searches – Galactic Center



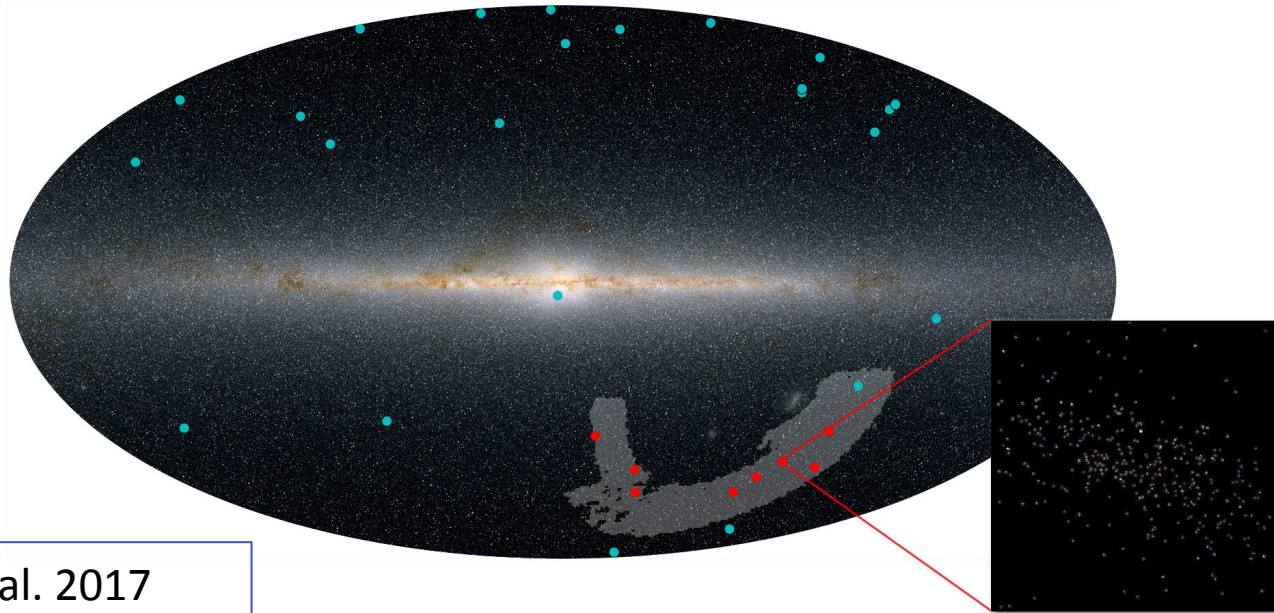
Ackermann, M. et al. 2017

Dark Matter searches – GC

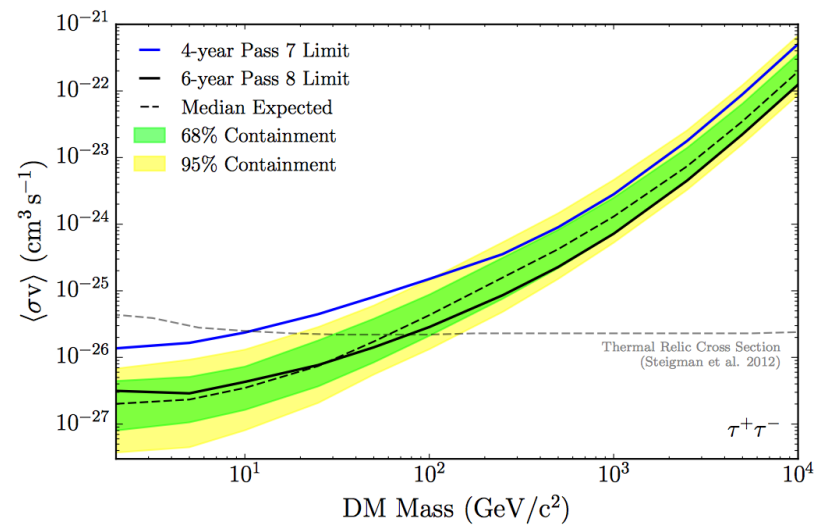
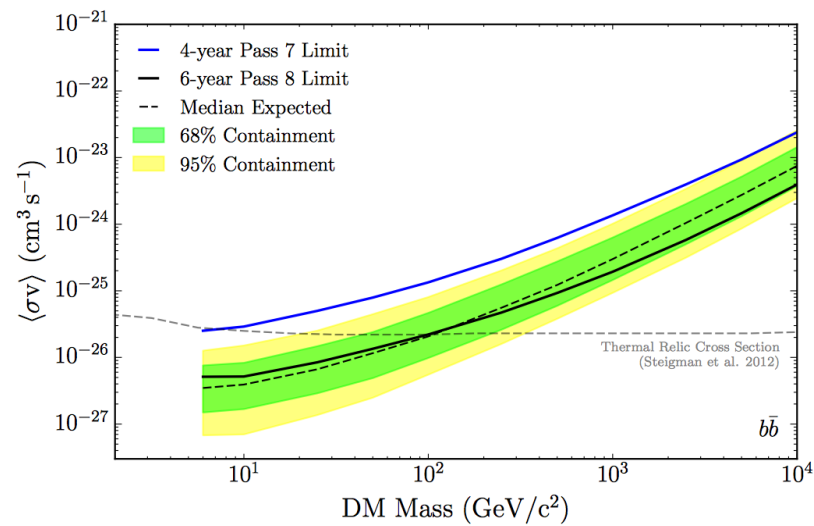


Ackermann, M. et al. 2017

Dark Matter searches – Dwarfs Galaxies



Albert, A. et al. 2017



How the LAT detects electrons

Trigger and downlink

Very versatile and configurable

- Triggering on ~ all particles that cross the LAT
 - Including electrons (8M/yr)

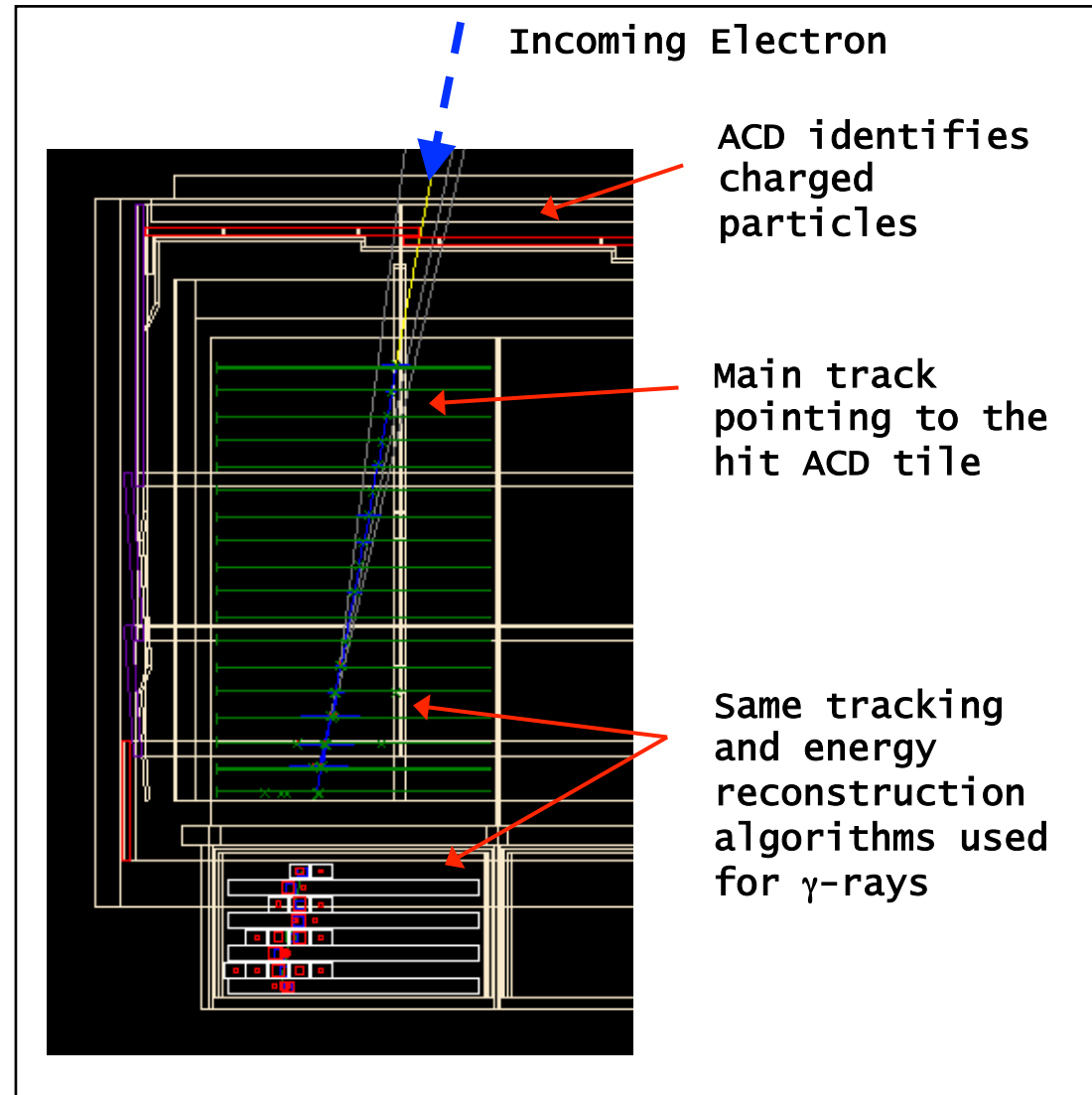
On board filtering to fit bandwidth

- Remove many charged particles
- Keeps all events with more than 20 GeV in the CAL (HE)
- Prescaled (1:250) sample of unfiltered triggers (LE)

Electron identification

The challenge is identifying the good electrons among the proton background

- Rejection power of $10^3 - 10^4$ required
- Can not separate electrons from positrons
- → Dedicated high energy electron event selection



Importance of a direct CRE measurement

- Probe CR models
 - Sources (including DM), interactions, propagation, diffusion
- Probe CR targets (ISM, ISRF)
 - Propagation and diffusion
 - Strong connection with diffuse gamma-ray radiation
- Probe possible nearby sources
 - limited electron lifetime within Galaxy
- Answers to long-standing questions and vast literature

THE ASTROPHYSICAL JOURNAL, 162:L181-L186, December 1970
© 1970. The University of Chicago. All rights reserved. Printed in U.S.A.

PULSARS AND VERY HIGH-ENERGY COSMIC-RAY ELECTRONS

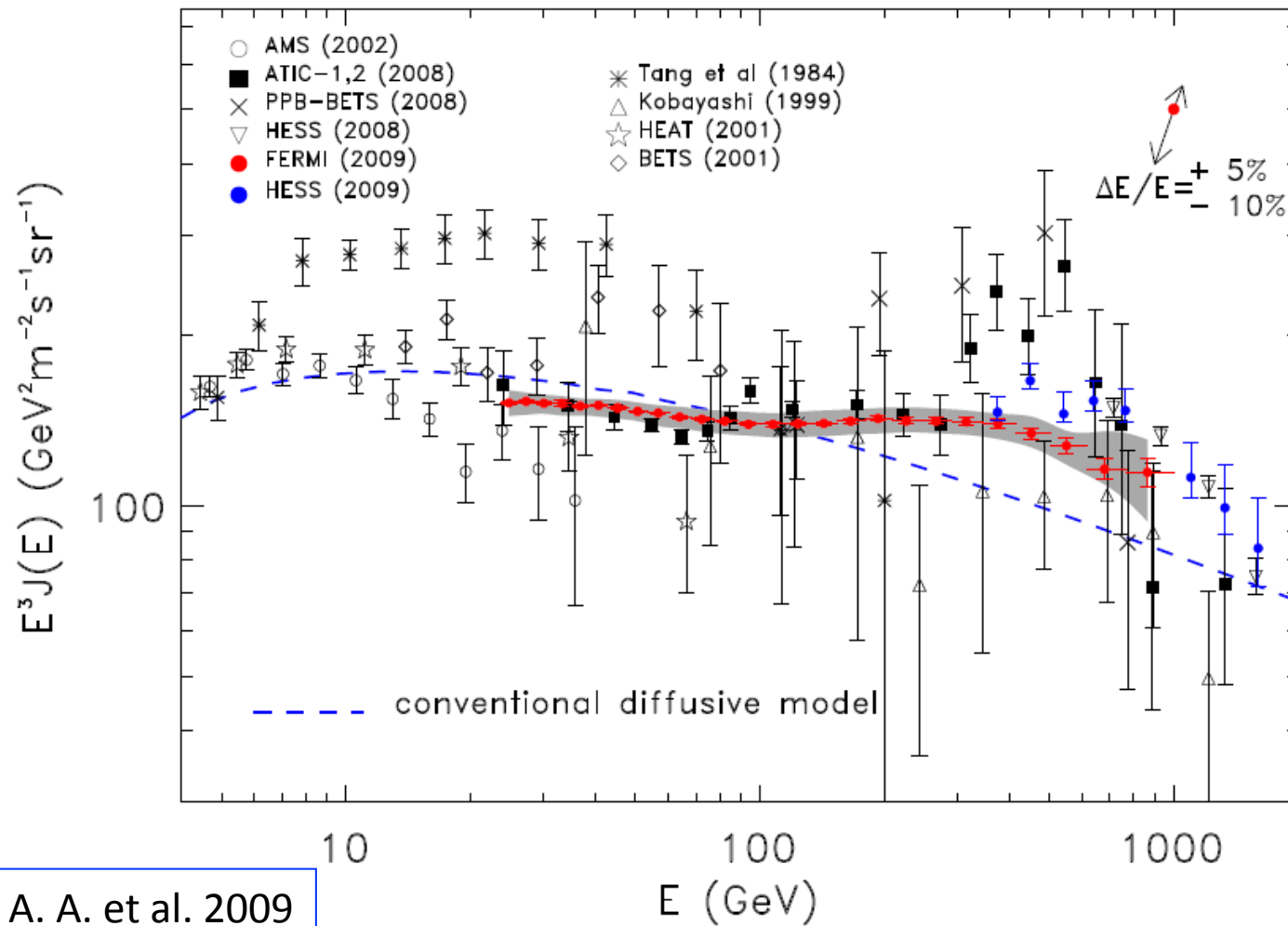
C. S. SHEN*

Department of Physics, Purdue University, Lafayette, Indiana 47907

Received 1970 June 8; revised 1970 September 19

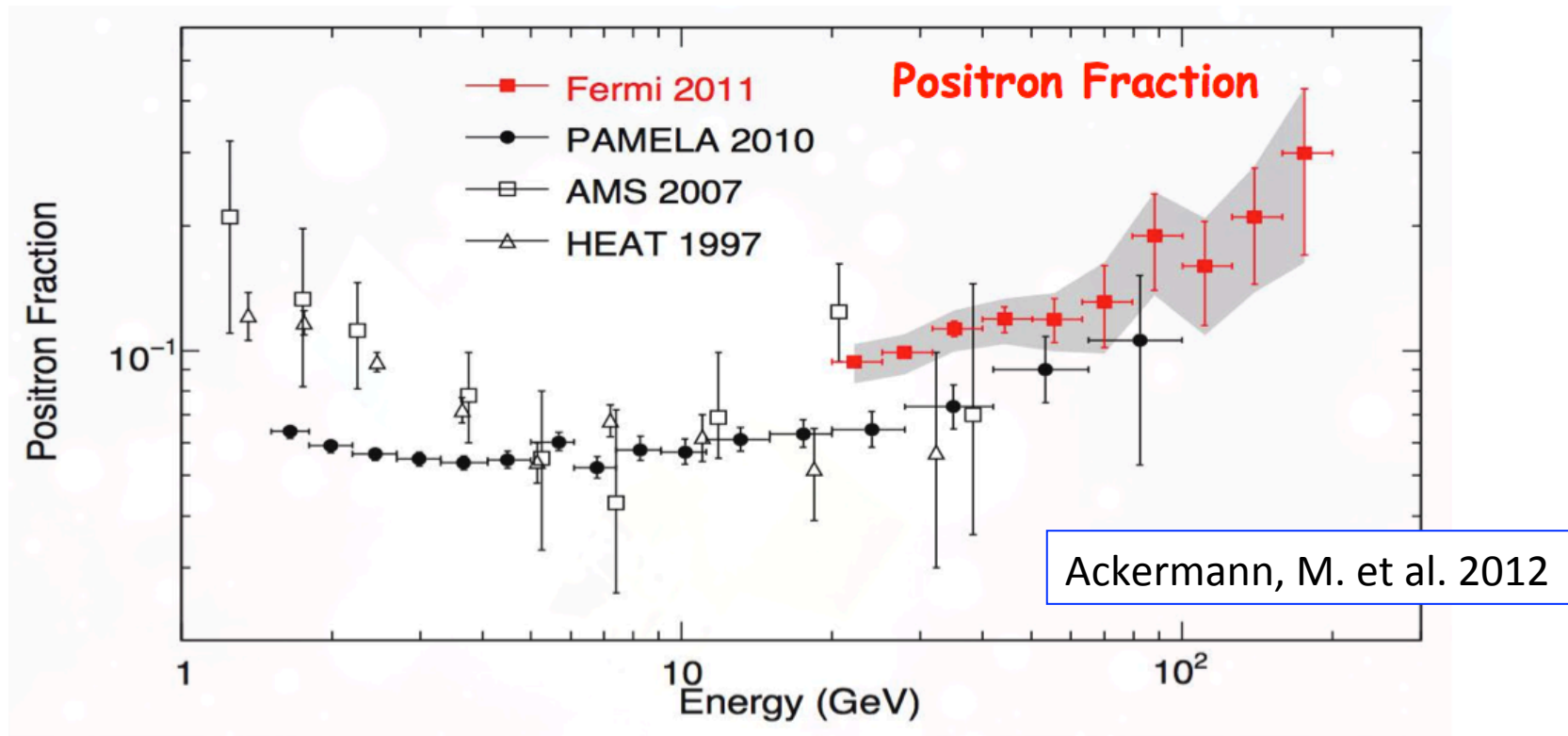


Measurement of the Cosmic Ray $e^+ + e^-$ Spectrum from 20 GeV to 1 TeV with the Fermi Large Area Telescope



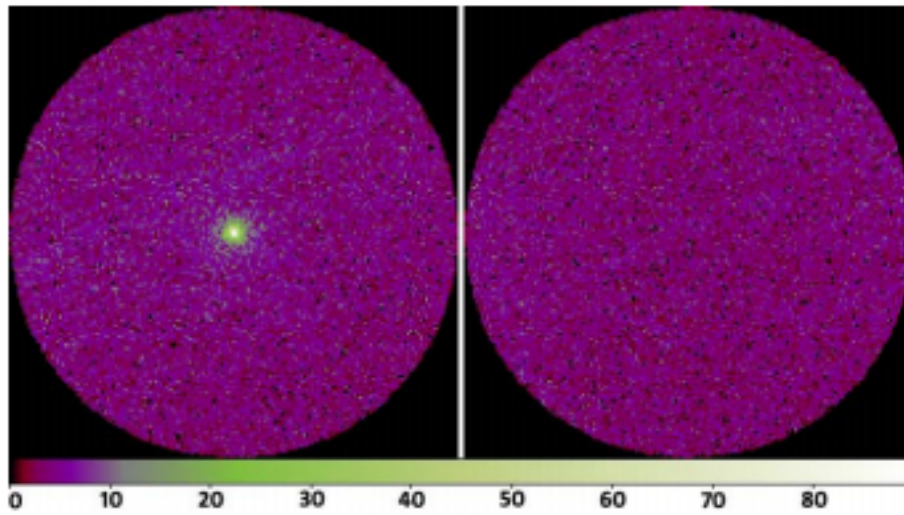
Abdo, A. A. et al. 2009

Positron Fraction Measurements

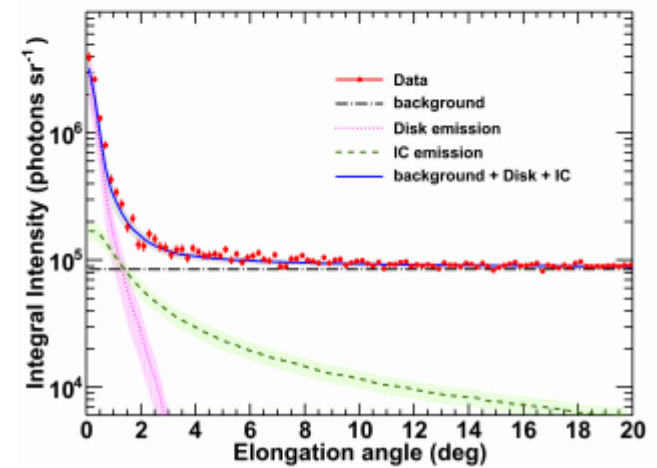
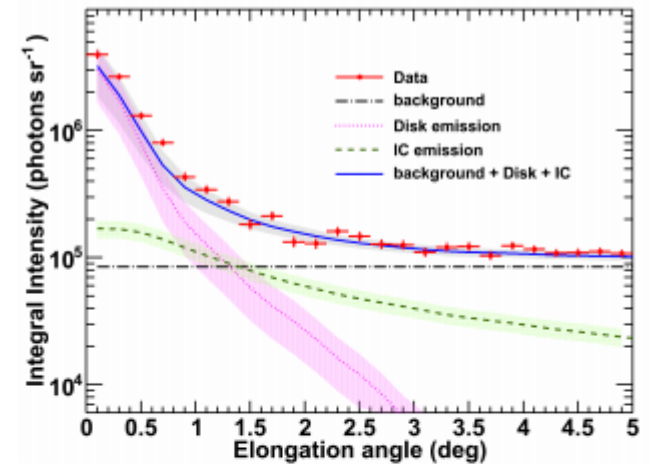


- PAMELA and Fermi-LAT observe a rise in local e^+ fraction above ~ 10 GeV
- This disagrees with conventional models (e.g., GALPROP) for cosmic rays (secondary e^+ production only)
- No similar rise is seen in anti-proton fraction

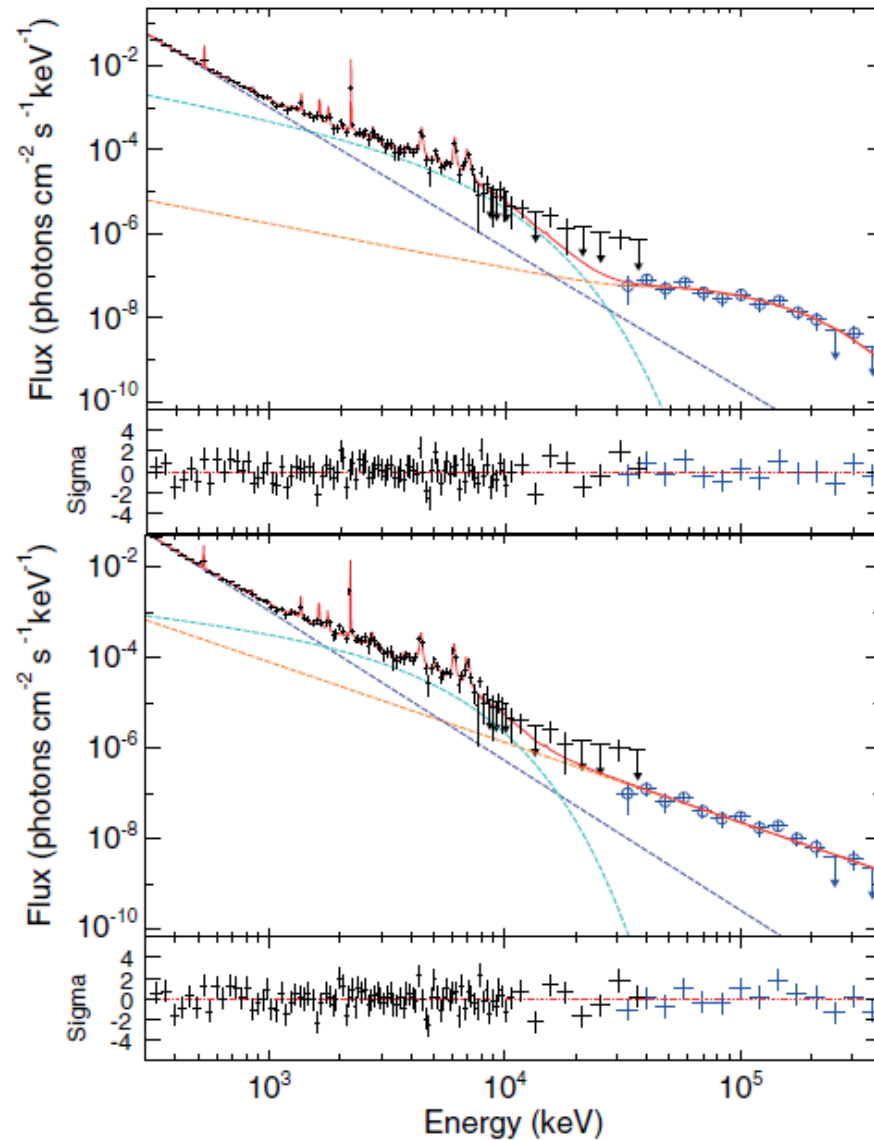
The Quiet Sun



Abdo, A. A. et al. 2011

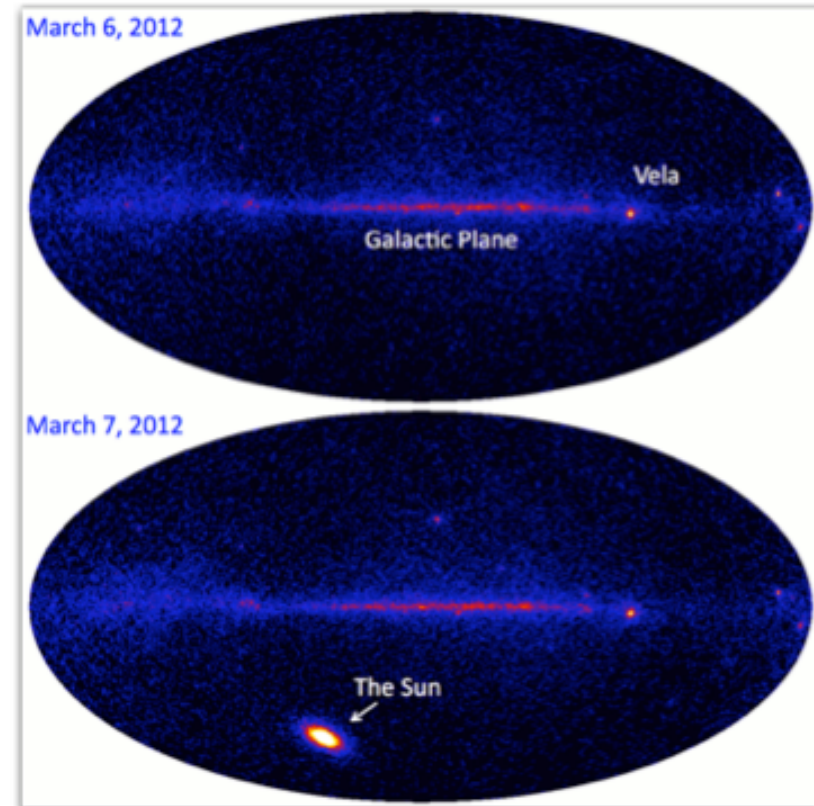
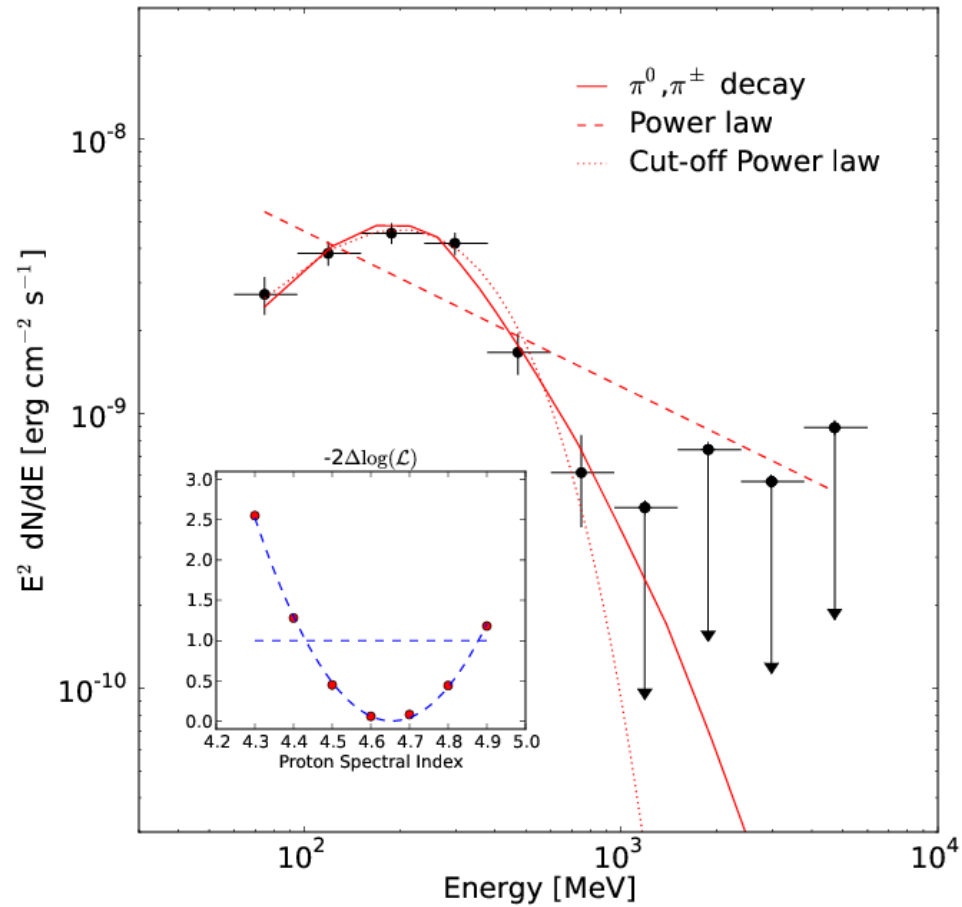


Challenge #5: Flaring Sun



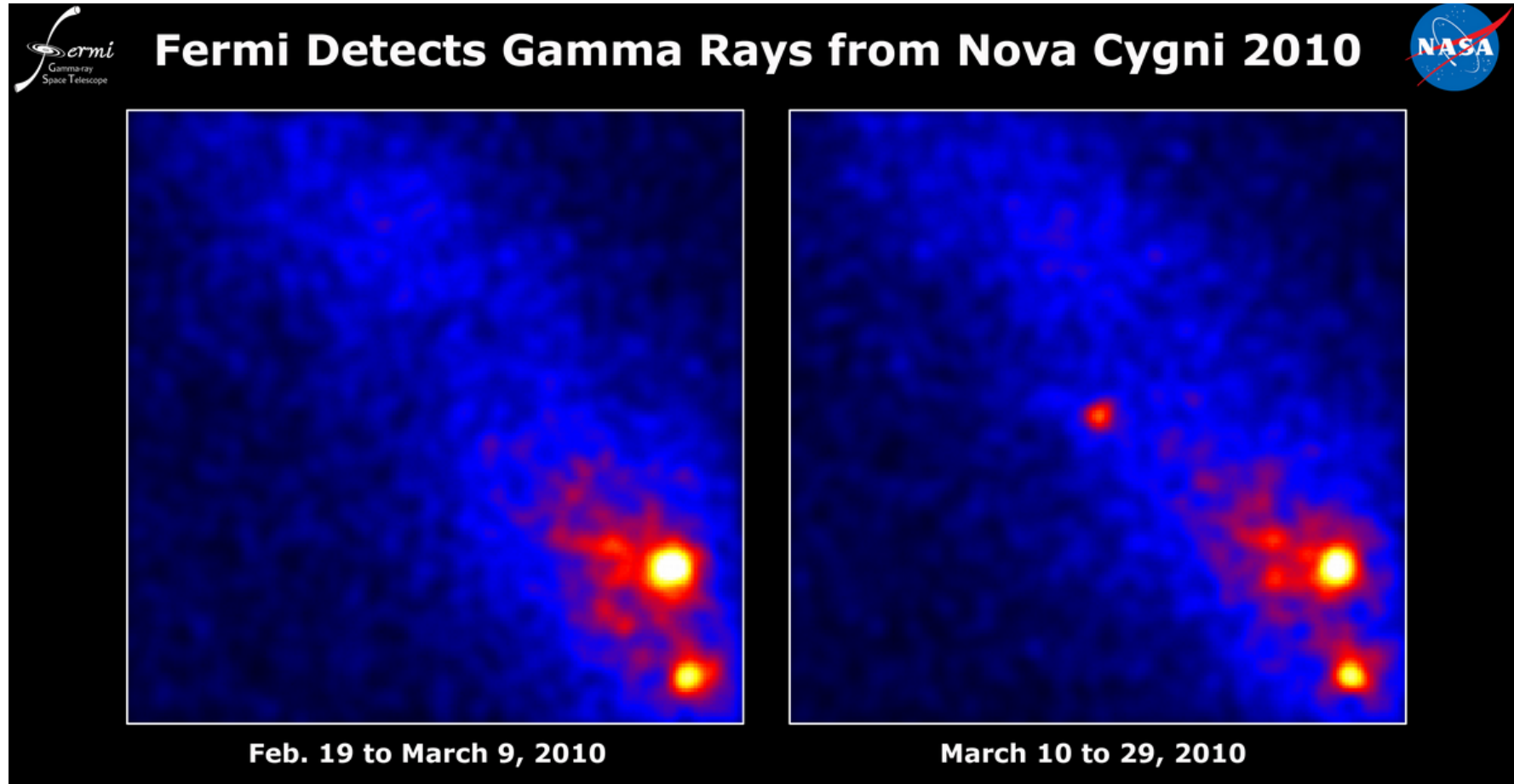
Ackermann, M. et al 2012

Solar Flares



Ajello, M. et al. 2014

Surprise! Nova emitting in Gamma Rays!



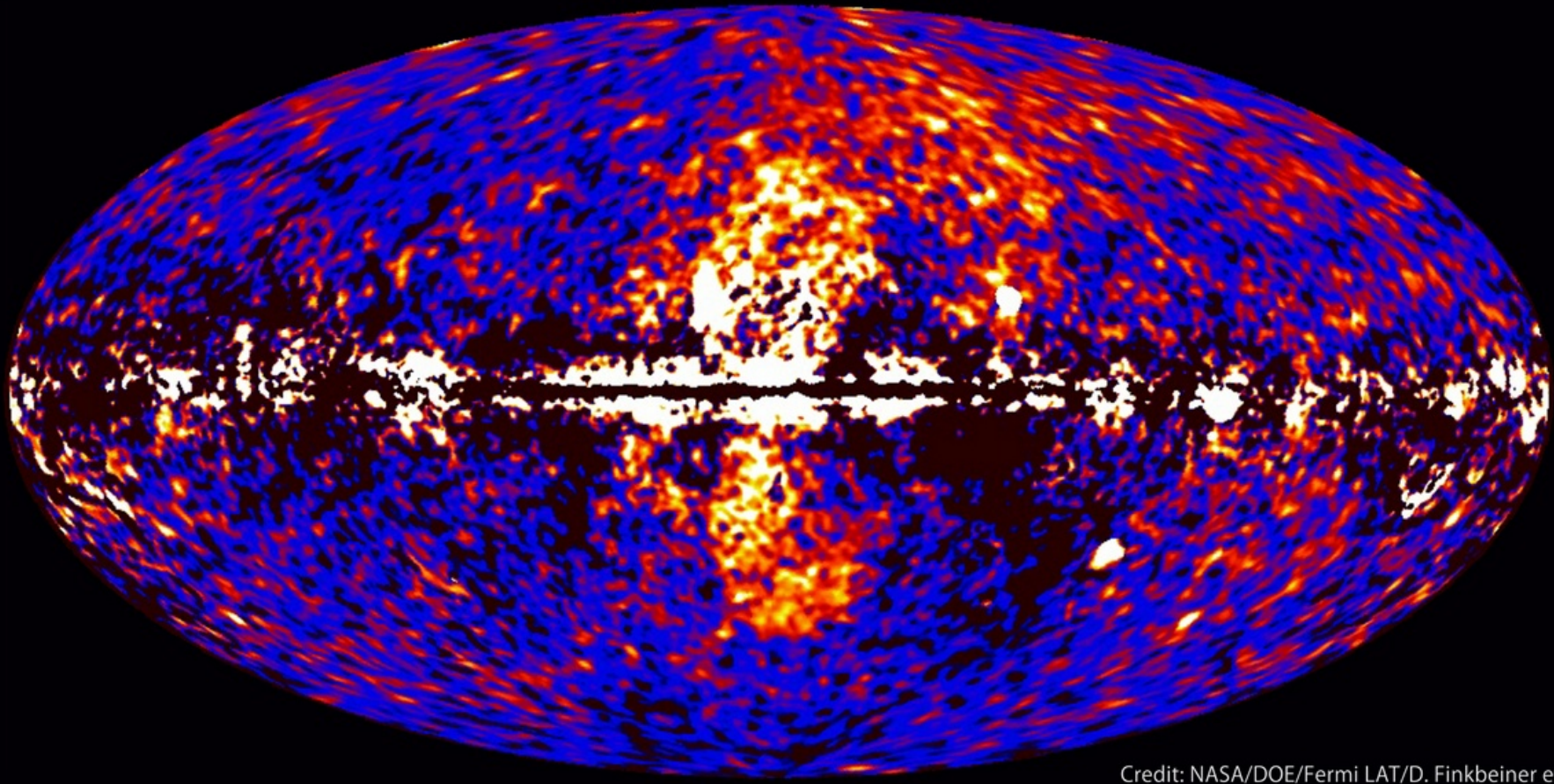
Abdo, A. A. et al. 2010

Gamma Ray Novae



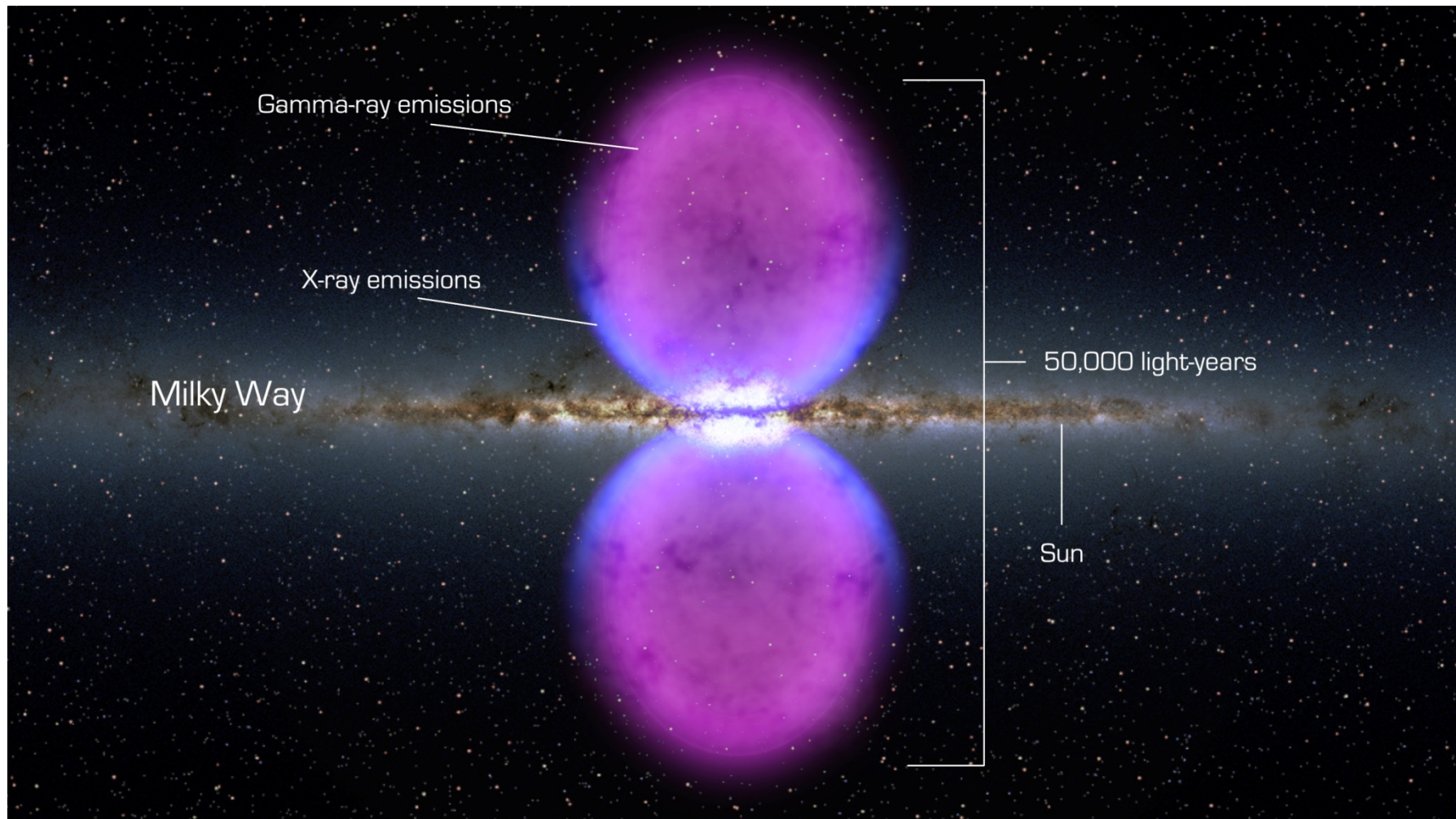
Surprise! The Fermi Bubbles

Fermi data reveal giant gamma-ray bubbles



Credit: NASA/DOE/Fermi LAT/D. Finkbeiner et al.

Fermi bubbles



LAT team analysis: Ackermann, M. et al. 2017

CALET?

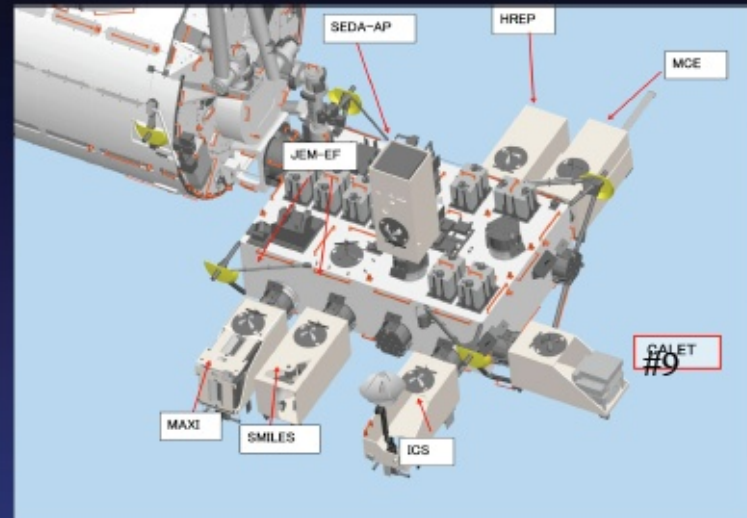
CALorimetric Electron Telescope (CALET)

P. S. Marrocchesi for the CALET Collaboration – RICAP11 – 2011 May 26

- **Instrument:**
High Energy Electron and Gamma-Ray Telescope
- **Carrier:**
HTV: H-IIA Transfer Vehicle
- **Attach Point on the JEM-EF: #9**
for heavy (< 2000 kg) payloads
- **Nominal Orbit:**
407 km, 51.6° inclination
- **Launch plan:**
FY 2013
- **Life Time:**
≥ 5 years



Firenze
Pisa
Siena
Roma Tor Vergata



1 GeV ~ 20 TeV for electrons

20 MeV ~ TeV for gamma-rays

Weight: 500 kg

GF (fiducial volume): ~ 0.12 m²sr

Power Consumption: 640 W

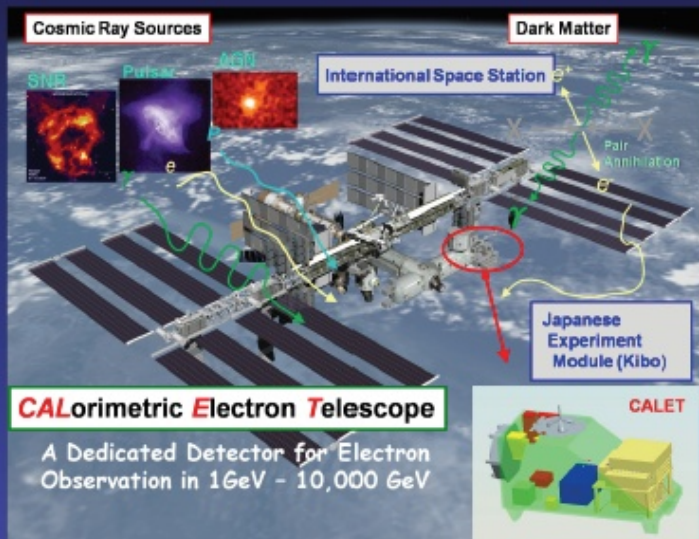
Data Rate: 300 kbps

CALET?

CALET Overview

Observation

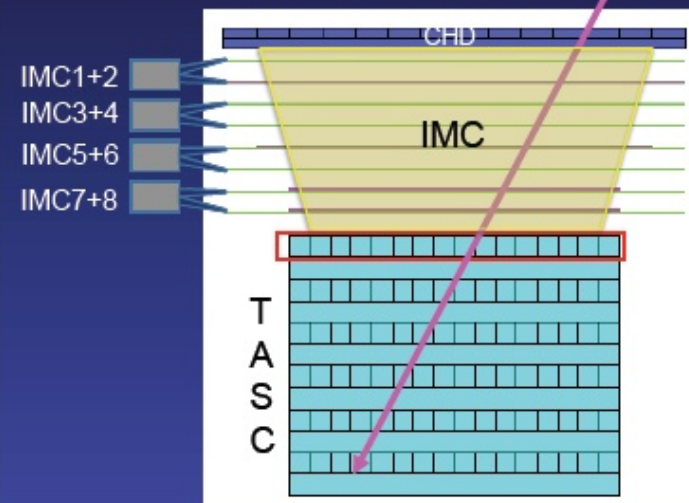
- **Electrons** : 1 GeV - 10 TeV
- **Gamma-rays** : 10 GeV-10 TeV (GRB > 1 GeV)
+ Gamma-ray Bursts : 7 keV-20 MeV
- **Protons, Heavy Nuclei**:
several 10 GeV- 1000 TeV (per particle)
- **Solar Particles and Modulated Particles**
in Solar System: 1 GeV-10 GeV (Electrons)



Instrument

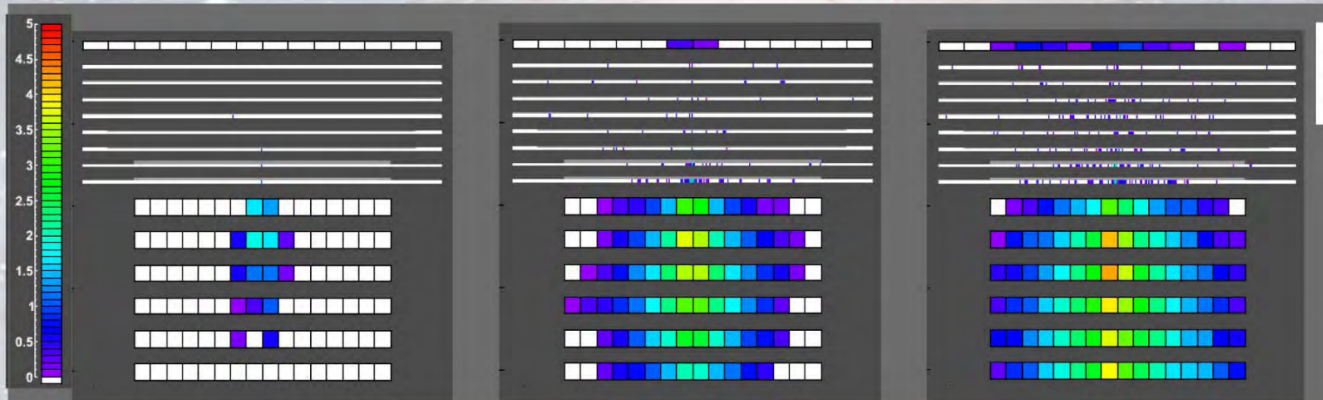
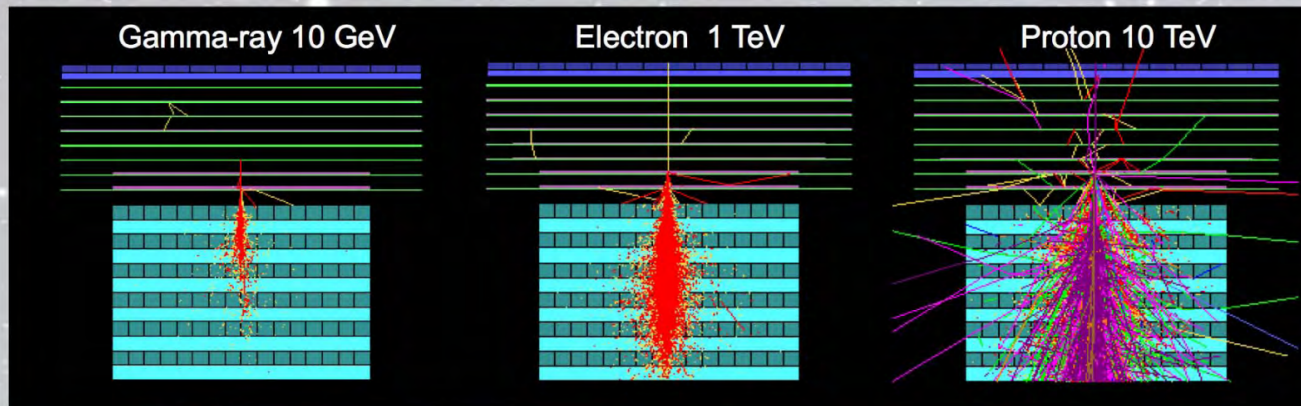
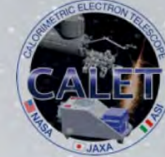
High Energy Electron and Gamma-Ray Telescope:

- **CHARGE DETECTOR (CHD)**
(Charge Measurement in $Z=1-40$)
- **IMAGING CALORIMETER (IMC)**
(Particle ID, Direction)
Total Thickness of Tungsten (W): $3 X_0$ 0.11 λ_T
Layer Number of Scifi Belts: 8 Layers * $2(X,Y)$
- **TOTAL ABSORPTION CALORIMETER (TASC)**
(Energy Measurement, Particle ID)
PWO 20mm x 20mm x 320mm
Total Depth of PWO: $27 X_0$ (24cm) , 1.35 λ_T



CALET

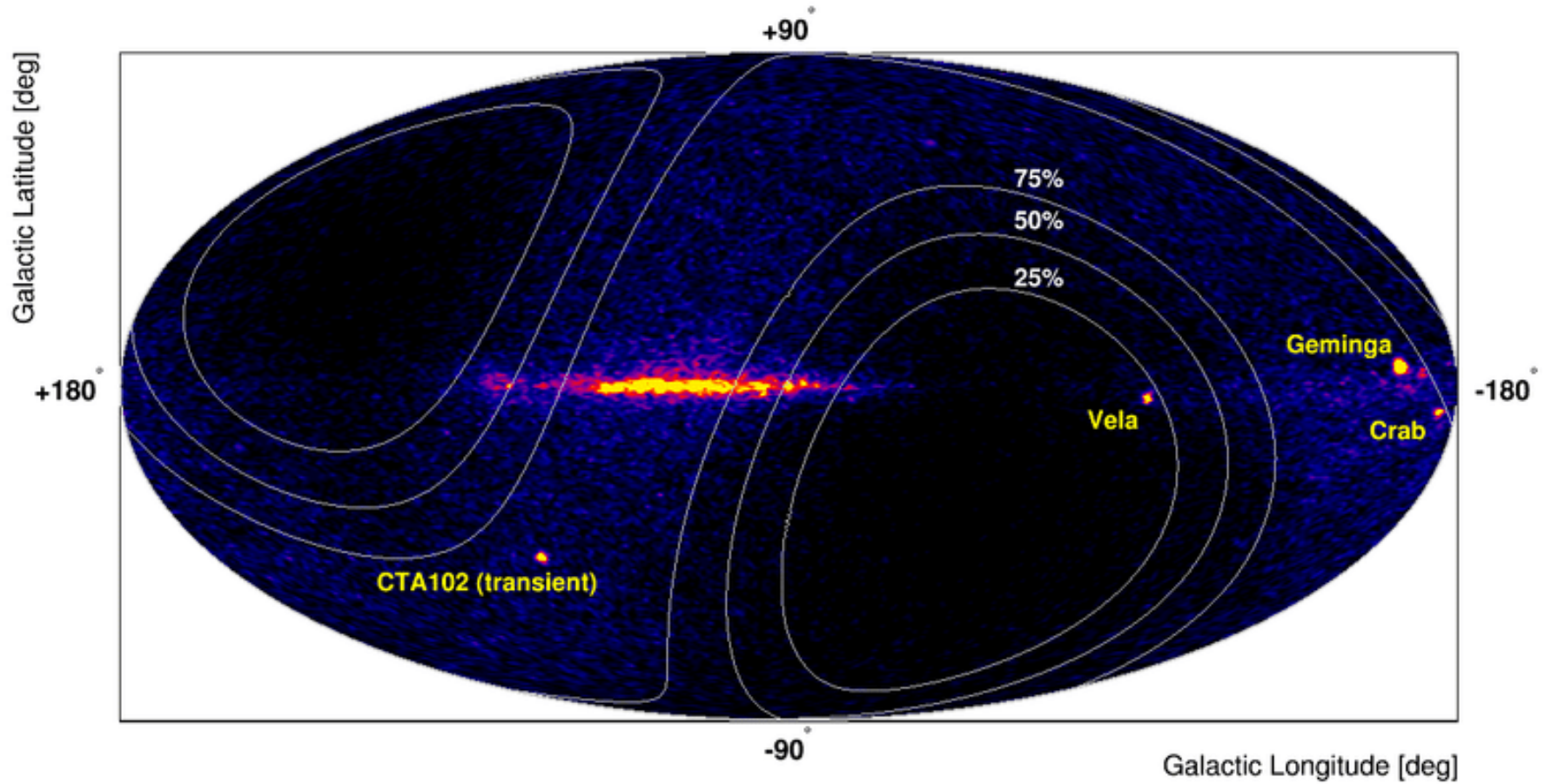
CALET/CAL Shower Imaging Capability (Simulation)



In Detector Space

- Proton rejection power $> 10^5$ can be achieved with the IMC and TASC shower imaging capability.
- Charge of incident particle is determined to $\Delta Z = 0.15 - 0.3$ with the CHD.

CALET gamma-sky



Gamma-400?

AC - anticoincidence detectors

C - multilayer converter

C1- C6 6 x 0,14Xo W

CD1 - CD6 6 x Si (x,y) strip
detectors (pitch 0.1 mm)

CD7 - CD8 Si (x,y) strip
detectors (pitch 0.1 mm)

S1, S2 - TOF detectors

TRD - transition radiation detectors

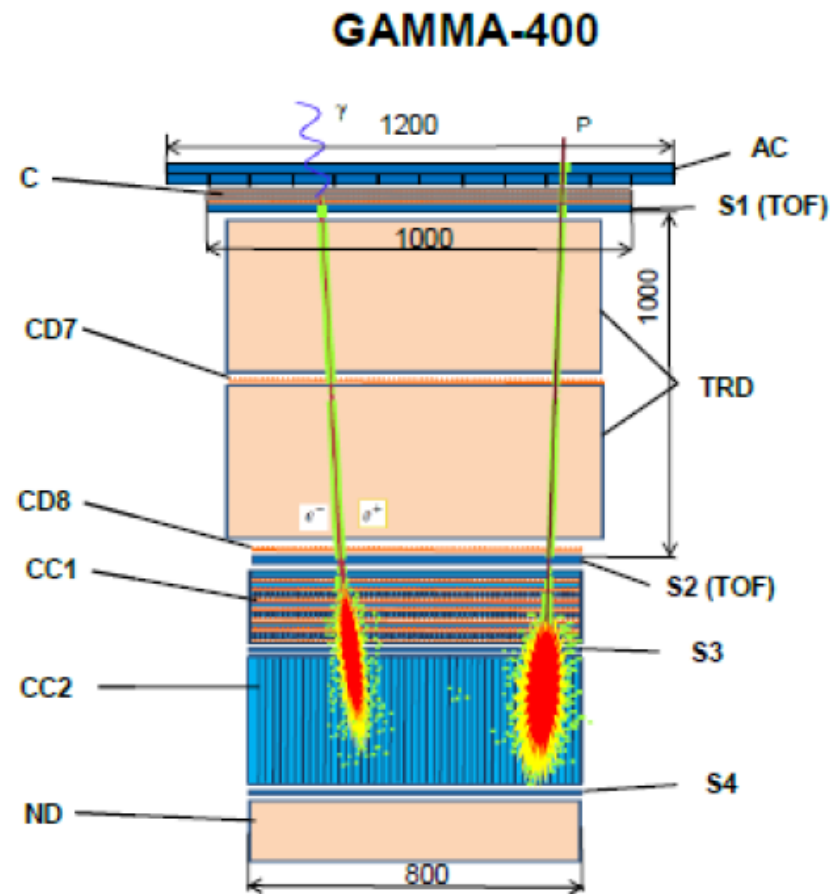
CC1 - imaging calorimeter (9Xo)

10 layers BGO + Si (x, y) strip
detectors (pitch 0.5 mm)

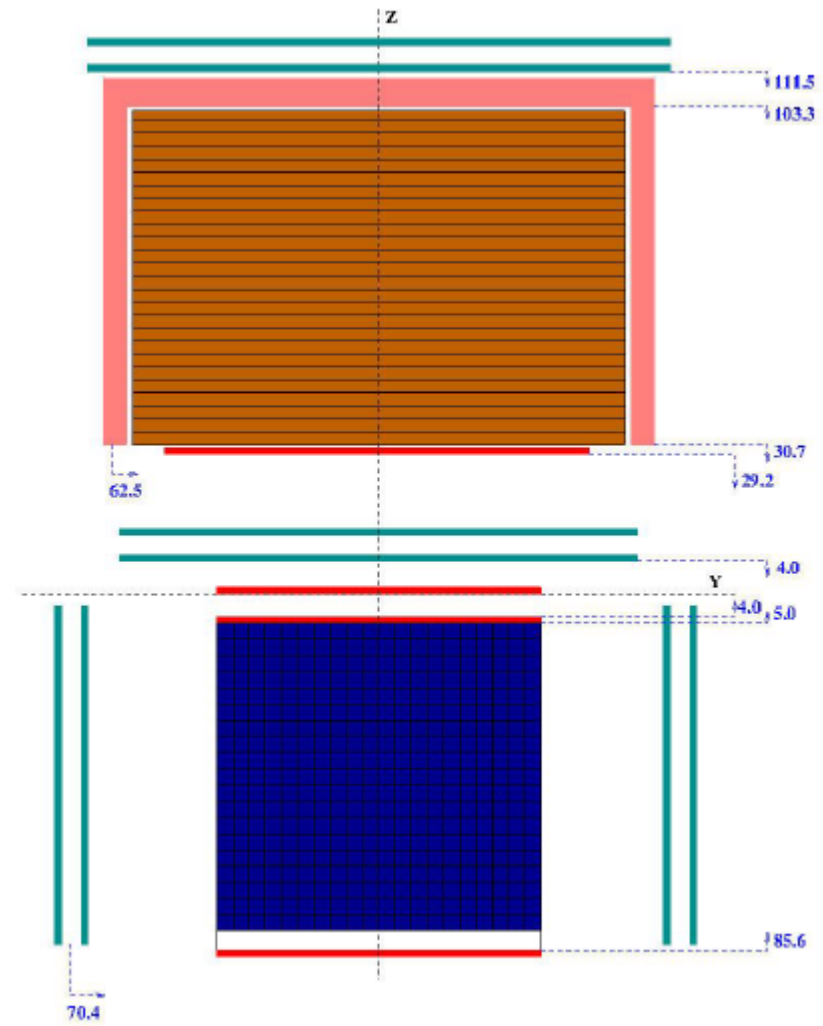
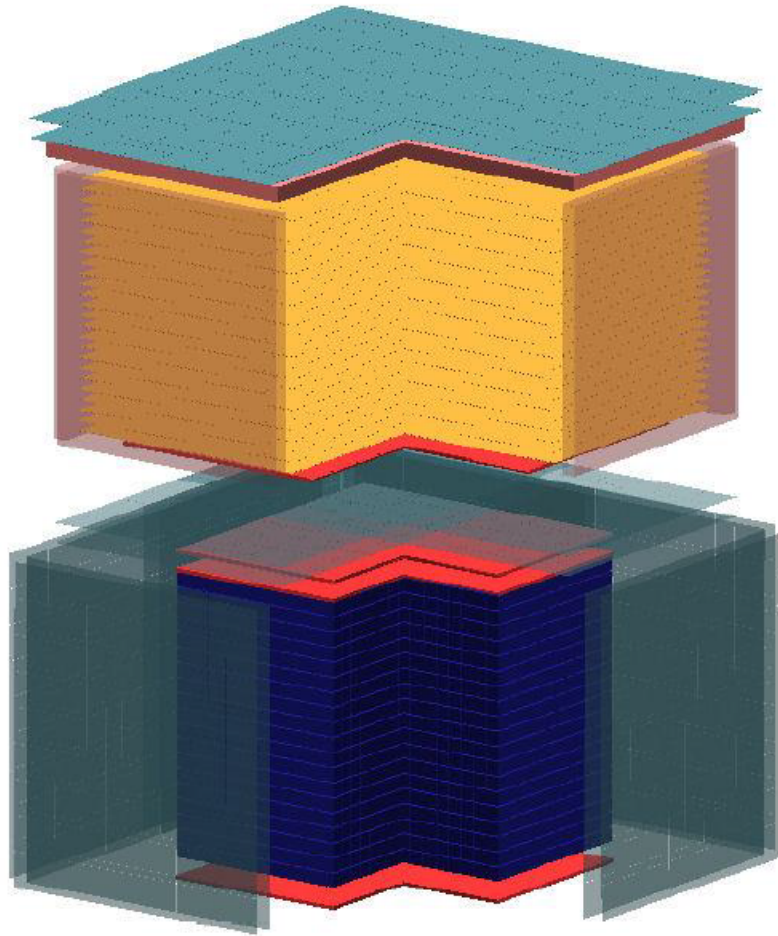
CC2 - BGO imaging calorimeter
(21.5Xo)

S3, S4 - scintillator detectors

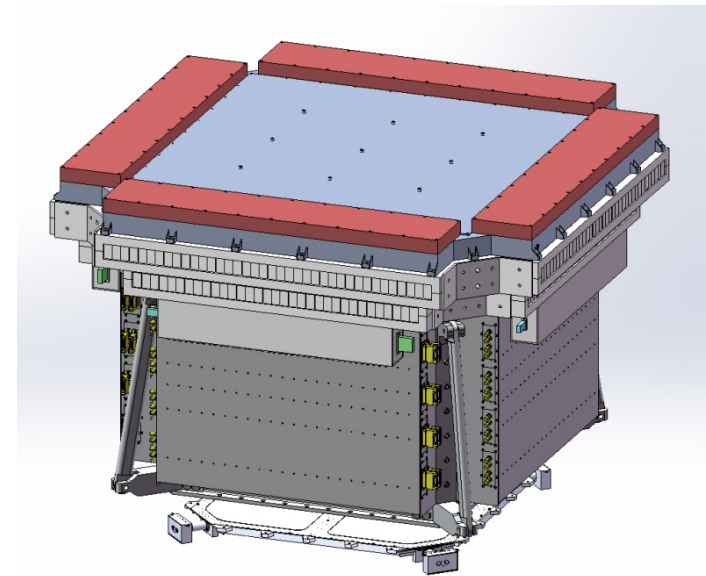
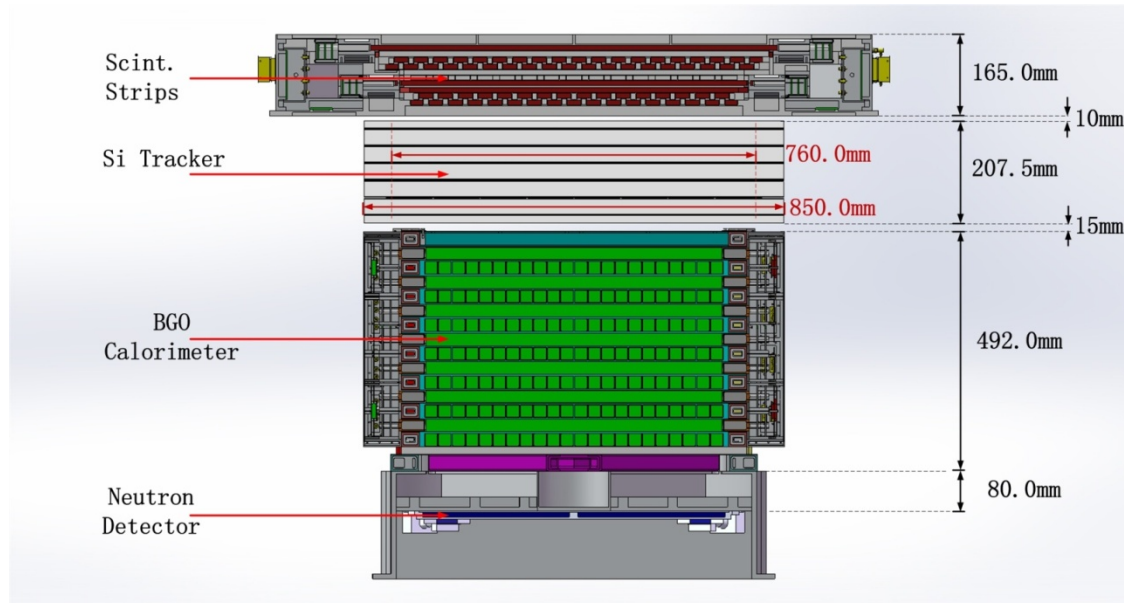
ND - neutron detectors



Gamma400



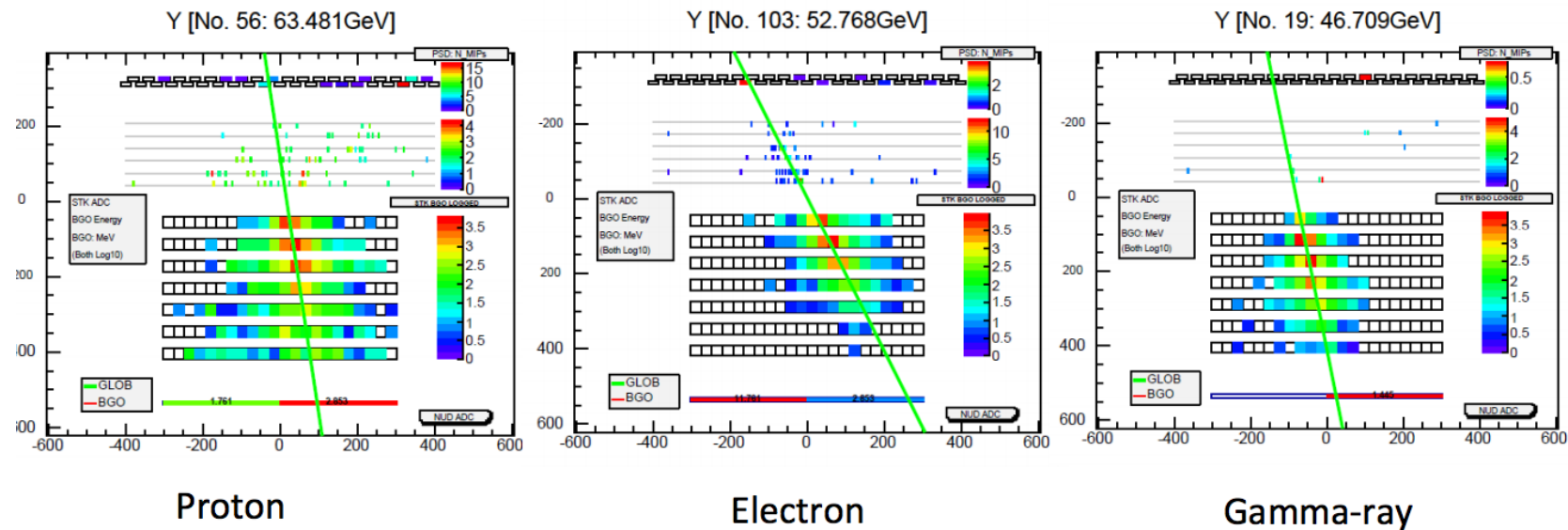
DAMPE



The detector is consisted of 4 parts:
Top scintillators (charge measurement)
Si tracker (5 layers)
BGO calorimeter
Neutron detector

DAMPE Gamma results

DAMPE γ -ray Selection: Different Events



- $e(\gamma)/p$ separation: BGO shower pattern
- e/γ separation: PSD and STK charge measurement

DAMPE Gamma results

DAMPE γ -ray Sky Map (Counts)

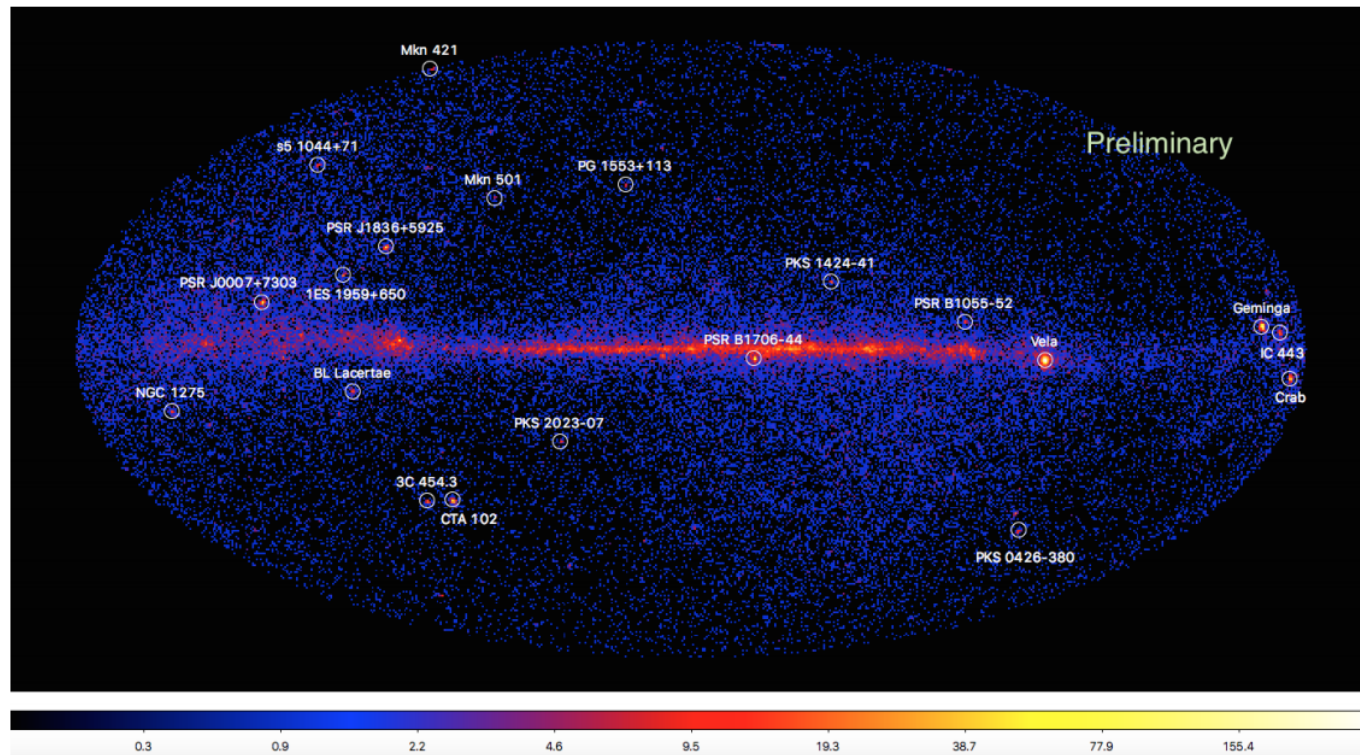
➤ 510 days

➤ $E > 2$ GeV

➤ 90,000
events

➤ $0.5^\circ \times 0.5^\circ$
pexel

➤ Mollweide
projection



HERD



Baseline Design: ~2 T, ~2 KW

Charge detector: Si+PIN.

Top: $2 \times (70 \times 70 \times (1 \text{ cm} \times 1 \text{ cm} \times 500 \mu\text{m}))$;

Sides: $4 \times (2 \times (70 \times 40 \times (1 \text{ cm} \times 1 \text{ cm} \times 500 \mu\text{m})))$

Shower Tracker:

W: $4X_0$; $10 \times 3.5 \text{ mm} +$

$2 \times 17.5 \text{ mm} + 2 \times 35 \text{ mm}$

Scin. Fibers:

$14 \times (2 \times (700 \times (1 \times 1 \times 700 \text{ mm}^3)))$

Nucleon Tracker: scin. fibers

$400 \times (1 \times 1 \times 700 \text{ mm}^3) +$

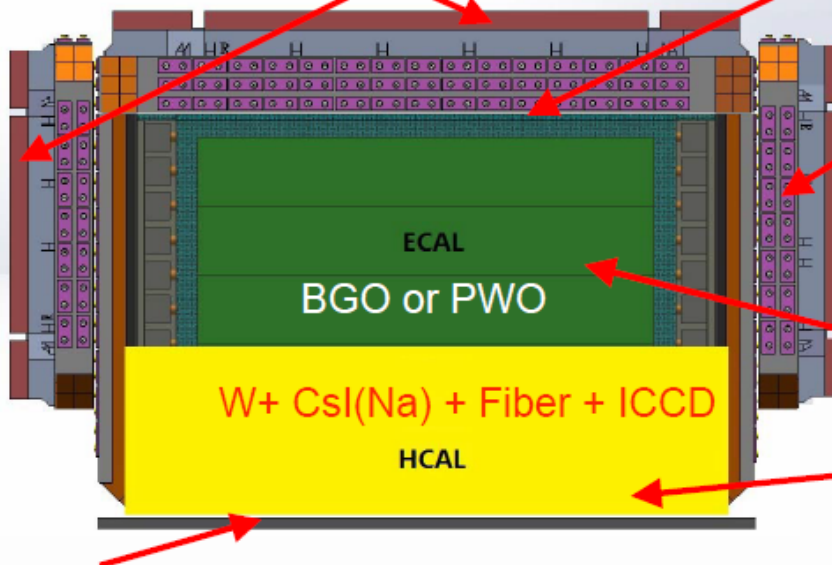
$700 \times (1 \times 1 \times 400 \text{ mm}^3)$

ECAL: $16X_0 = 0.7X_{\text{NIL}}$

$3 \times (2 \times (25 \times 25 \times 700 \text{ mm}^3))$

HCAL: W: $20 \times 3.5 \text{ mm} (0.8X_{\text{NIL}})$

CsI: $20 \times (2.5 \text{ cm} \times 2.5 \text{ cm} \times 0.2 \text{ cm})$



Neutron detector: B-doped plastic scintillator for delayed signals. Enhanced e/p discrimination. (TBD)



中国科学院空间科学与应用总体部

GENERAL ESTABLISHMENT OF SPACE SCIENCE AND APPLICATION,
CHINESE ACADEMY OF SCIENCES

Scientific Highlights of the LAT

National Aeronautics and Space Administration



Fermi's Decade of Gamma-ray Discoveries

Fermi 10-year Sky Map

This all-sky view, centered on our Milky Way galaxy, is the deepest and best-resolved portrait of the gamma-ray sky to date. It incorporates observations by NASA's Fermi Gamma-ray Space Telescope from August 2008 to August 2018 at energies greater than 1 billion electron volts (GeV). For comparison, the energy of visible light falls between 2 and 3 electron volts. Lighter shades indicate stronger emission.

NASA/DOE/Fermi LAT Collaboration

GRB 130427A

On April 27, 2013, a burst of light from a distant galaxy became the focus of astronomers around the world. The explosion, known as a gamma-ray burst, and designated GRB 130427A, was detected by Fermi for about 20 hours. The burst included a 95 GeV gamma ray, the most energetic light yet detected from a GRB.

NASA/DOE/Fermi LAT Collaboration

Solar Flare

Although our Sun is not usually a bright gamma-ray source, solar flares can briefly outshine everything else in the gamma-ray sky. On March 7, 2012, Fermi detected flares erupting on the side of the Sun not visible to the spacecraft. The flares produced accelerated particles that fell onto the side of the Sun-facing Earth, resulting in gamma rays Fermi could detect.

NASA/DOE

PSR J1744-7619

Discovered by Einstein@Home, a distributed computing project that analyzes Fermi data using home computers, PSR J1744-7619 is the first gamma-ray millisecond pulsar that has no detectable radio emission.

NASA/DOE/Fermi LAT Collaboration/SSU/A. Siemsen et al.

ASASSN-16ma

Fermi has discovered several novas, outbursts powered by thermonuclear explosions on white dwarf stars. This was a surprise because novas weren't expected to be powerful enough to produce gamma rays. One event, dubbed ASASSN 16ma, shows that both gamma rays and visible light seem to be produced by the same physical process.

NASA/DOE/Fermi LAT Collaboration

GRB 170817A

This landmark event represents the first time light was seen from a source that produced gravitational waves. Fermi's detection of GRB 170817A coincided with a signal from merging neutron stars detected by the LIGO and Virgo gravitational-wave observatories.

ASTRO2017/DOE/SSU/AMC/MSM

TXS 0506+056

Among the nearly 2,000 active galaxies Fermi monitors, TXS 0506+056 stands out as the first one known to have produced a high-energy neutrino. Neutrinos are tiny, ghost-like particles that barely interact with matter and are thought to be produced in the same extreme physical environments as gamma rays. In July 2018, Fermi linked this galaxy to a detection by the IceCube Neutrino Observatory at the South Pole.

NASA/DOE/Fermi LAT Collaboration



Fermi Bubbles

Fermi data revealed vast gamma-ray bubbles extending tens of thousands of light years from the Milky Way's plane. The Fermi Bubbles may be related to past activity of the supermassive black hole at our galaxy's heart.

NASA/Goddard

Galactic Center

The central region of the Milky Way is brighter in gamma rays than expected. Whether this excess is a collection of undiscovered millisecond pulsars or possibly evidence of annihilation of dark matter particles remains a mystery and will be part of Fermi's ongoing studies.

NASA/Goddard/A. Mellinger, CMU, T. Linden, Univ. of Chicago

IC 443, the Jellyfish Nebula

The shock waves of supernova remnants like the Jellyfish Nebula can accelerate protons to near the speed of light. When they slam into nearby gas clouds, gamma rays are produced. Fermi detects this emission, confirming that supernova remnants accelerate high-energy cosmic rays.

NASA/DOE/Fermi LAT Collaboration/DOE/SLAC/PS-Catena/USCLA

Crab Nebula

The Crab Nebula, a young supernova remnant radiating a pulsar, surprised Fermi astronomers with gamma-ray flares driven by the most energetic particles ever traced to a specific astronomical object. To account for the flares, scientists say electrons near the pulsar must be accelerated to energies a thousand trillion (10¹⁴) times greater than visible light.

NASA/CXC/NASA/MSU/Heiter et al.



Future Gamma-ray Experiments?

Scientific Motivations and Technical Design Considerations for Future High-Energy γ -ray Telescopes in Light of Lessons Learned from the Fermi Large Area Telescope.

Eric Charles^a

on behalf of the *Fermi* Large Area Telescope Collaboration

^aKavli Institute for Particle Astrophysics and Cosmology, SLAC National Accelerator Laboratory, 2575 Sand Hill Road, M/S 29 Menlo Park, CA 94025, USA;

ABSTRACT

Five years into the *Fermi Gamma-ray Space Telescope* (*Fermi*) mission we have learned a great deal about the γ -ray sky, yet many open questions remain, and many new puzzles have arisen. In this contribution we will consider the science drivers for a variety of topics in high-energy gamma-ray astronomy, and how these drivers map into design considerations for future gamma-ray instruments in the energy range above 5 MeV. Specifically, we take the performance parameters and data set of the Large Area Telescope on the *Fermi* observatory (*Fermi-LAT*) as a baseline, and consider the scientific questions that could be probed by improving those parameters. We will also discuss the current state of detector technologies used in space-based γ -ray telescopes and discuss the magnitude of advances that would be required to make a future *Fermi*-like mission transformational enough to warrant the cost and effort. These summaries are intended to be useful for selecting technologies and making basic design decisions for future γ -ray telescopes.

Table 1. Summary of the importance of instrument performance parameters for science topics in high-energy γ -ray astronomy. Key performance parameter are marked as “1”, other important parameters as “2”, marginally relevant parameters as “3” and irrelevant parameters are unmarked. The performance parameters are background rejection (“Bkg”), point-source sensitivity (“Source”), on-axis A_{eff} (“ A_{eff} ”), field-of-view (FOV), point-source localization (“PSF Loc.”), extension detection/ associating a given γ ray with a particular source (“PSF Ext.”), energy bandpass (“Band”), energy resolution (“Energy Res.”), spectral resolution (“Energy spec.”), relative timing and deadtime between readouts (“Timing Rel.”) and absolute timing (“Timing Abs.”).

Topic			Acceptance		PSF		Energy			Timing	
	Bkg.	Source	A_{eff}	FOV	Loc.	Ext.	Band	Res.	Spec.	Rel.	Abs.
GRB Detection	2	1	1	1	3	-	2	-	-	-	-
GRB Localization	2	2	2	2	1	-	-	-	-	-	-
GRB Modeling	2	2	1	1	-	2	1	2	1	2	3
GRB EBL Studies	2	3	1	1	-	2	2	2	-	-	3
GRB LIV Studies	3	-	1	1	-	2	2	2	-	1	2
AGN Pop. Studies	3	1	1	2	1	-	1	3	2	-	-
AGN Variability	3	1	1	1	-	-	2	3	2	-	-
AGN EBL Studies	3	1	1	2	-	1	2	3	3	-	-
Nearby Galaxies	3	1	1	2	3	1	1	3	2	-	-
Galactic Diffuse	1	2	2	2	-	1	3	3	2	-	-
Extra-Galactic Diffuse	1	2	2	2	-	2	1	3	2	-	-
Radio Timed Pulsars	3	1	1	1	-	2	2	3	2	3	1
Blind Search Pulsars	2	2	1	1	1	2	2	3	2	3	1
Pulsar Radio Targets	3	1	1	2	1	-	3	3	3	-	-
Pulsar Modeling	3	2	1	2	-	2	2	2	1	3	1
SNR / PWN	2	2	1	2	3	1	1	2	1	-	-
X-ray Binaries	2	1	1	2	2	3	1	3	2	-	-
Galactic Novae	2	1	1	2	1	3	1	3	2	-	-
Earth	-	-	3	2	-	3	1	3	1	-	-
Sun / Moon	2	1	1	2	3	1	1	3	2	-	-
Solar Flares	2	1	1	1	1	3	1	3	2	2	-
TGFs	-	-	2	2	-	-	3	-	-	1	2
DM dSph	2	1	1	2	-	2	2	3	2	-	-
DM Galaxy Clusters	2	1	1	2	-	1	2	3	2	-	-
DM Inner Galaxy	3	2	2	2	1	1	1	3	1	-	-
DM Lines	1	-	2	2	-	3	1	1	1	-	-

Design considerations

- Summary of interaction processes
 - Radiation Length
 - Pair conversion and Compton scatter
 - Energy Losses of Electrons and Positrons
 - Electromagnetic Shower Propagation
 - Multiple Coulomb Scattering
 - Plane thickness and Hit spacing

Implication for Instrument Performance

- Background rejection versus FOV.
- A_{eff} versus PSF.
- Sky-survey versus Pointed Observations
- PSF, Timing Resolution versus Power Budget.
- Energy Resolution versus A_{eff} and FOV.
- Size versus Complexity of Event Readout, Triggering and Filtering.
- Optimal Orbit.

Implication for Instrument Performance

Semiconductor-based solid state trackers. These include both strip and pixel detectors made from semiconductors such as silicon, germanium or diamond. All of these can achieve very precise positional accuracy, generally better than 30% of the channel pitch and as good as half that for detectors that use pulse height information to place hits between channels. Semiconductor detectors can also provide good measurements of the ionization energy deposited.

The limitation of these technologies are primarily geometrical. First, they they are generally built with thin flat planes, providing one measurement per plane (or two for double-sided detectors). The thickness of the planes is $> 200\mu m$, corresponding to $> 0.002X_0$ for particles at normal incidence, and increasing as the \cos^{-1} of the incidence angle. Furthermore, the semiconductor wafers require support structures, increasing the X_0 per measurement. Second, they achieve high precision by having extreme segmentation, and the number of readout channels can grow very large and present challenges for the power and thermal budget and the available data transmission bandwidth (see Sec. 4.2). The 18 bi-layer LAT has 884k channels. Building an instrument with 200 layers of $0.005X_0$ each for a total of $1X_0$ of conversion target would increase that 100-fold. Furthermore, with the LAT's spatial resolution of $\sim 70\mu m$ the layers would need to be placed at least 2 cm apart to avoid degrading the PSF at 100 MeV. This would result in a 4 m tall instrument.

Implication for Instrument Performance

Time Projection Chambers. TPCs work by using a near uniform electric field to drift charge carriers produced by ionization to the sides of the detector, where they are read out by sensor pads, which provide positional information in both direction transverse to the drift direction. Positional information in the longitudinal direction comes from measuring the drift time of the charge carriers.

Advances in solid-state sensor technology have made it possible to build very small individual channels on the amplification and sensor pads, allowing for excellent ($50\mu\text{m}$ or better) resolution in the transverse directions. However, the diffusion of the charge carriers limits the positional resolution in the longitudinal direction, particularly for large gas TPCs. With careful tuning of the drift gas longitudinal resolutions of $< 200\mu\text{m}$ for 1 m scale TPCs have been achieved.

TPCs can also quantify the ionization, which is useful for particle identification and quantifying the energy lost by charge particles in the TPC. The latter is particularly important for reconstructing Compton-scattering events.

One advantage of gas TPCs is that the density of the gas is low enough that several position measurement can contribute to the direction measurement, giving an excellent PSF. Furthermore, the density can be tuned to optimize the X_0 per-measurement. However, even the densest gases would require extreme pressures to provide enough target material for pair-conversion to reach LAT-like level; e.g., using Xe would require 50 bar of pressure at 300 K to reach $1X_0/\text{m}$. This suggests either segmented TPC cells with converter material between them, or placing converter material in the TPC.

Gas TPCs have other potential disadvantages. 1) The lower resolution in the longitudinal direction. 2) The difficulties in keeping the gas tuned for optimal performance. 3) The degradation of the gas and the readout sensor from chemical interaction between the two. 4) The difficulties in operating high-pressure gas systems in orbit. These last two suggest that the drift gas is potentially a mission-limiting consumable. On the other hand, it is worth noting that gas-based detection systems have been used successfully in several mission.

Solid-state (i.e., drift-detectors) or liquid TPCs offer less flexibility in tuning the X_0 per-measurement, but are also somewhat less difficult to operate in orbit. However, it is worth noting that liquid Ar (as in LArGO) requires substantial cooling, potentially creating a mission-limiting consumable or increasing the heat load on the spacecraft radiators.

Implication for Instrument Performance

Hodoscopic Crystal Calorimeters Calorimeters for pair-conversion γ -ray mission have been homogeneous high-Z scintillating crystals. For ground-based calorimeters where the shower is largely contained, the energy resolution is usually parametrized as:

$$\frac{\sigma_E}{E} = \frac{a}{\sqrt{E}} \oplus b \oplus \frac{c}{E}, \quad (12)$$

where the first term represents stochastic and sample fluctuations, the second term comes from the calibration uncertainties, and the third term from the electronics noise in the channels contributing to the shower. Typical ground-based electromagnetic have 15 to 20 X_0 , and can achieve resolutions as good as $2\%/\sqrt{E/1\text{GeV}}$. Mass constraints for space missions coupled with the generally smooth spectra of astrophysical sources in the GeV range suggest using somewhat thinner calorimeters. The LAT, for example, is only $8.6X_0$ at normal incidence, and achieves energy resolution of better than 10% from 1 GeV to 100 GeV. Once the shower-maximum (Eq. (8)) is beyond the calorimeter depth, Eq. (12) breaks down with increasing energy.

Plastic Scintillators. Plastic scintillators are efficient, low-cost detectors. They have been used successfully as anti-coincidence charged particle vetoes in several γ -ray telescopes, and can provide particle background rejection factors better than to 10^4 . Furthermore, the LAT has shown that segmenting the veto system can avoid “self-veto” from backslash particles in high-energy γ -ray events.

As mentioned in Sec. 3.5, very high rates of X-rays are observed in the LAT ACD during bright solar flares. This raises the possibility of designing the readout system of any veto system so that it can double as a bright transient detector and spectrograph.

Discussion

Optimizing the PSF. The largest potential gains in many science areas come from improving the PSF, particularly at the lower energies in the MCS dominated regime (< 1 GeV). Furthermore, no space-based instrument can feasibly compete with CTA above ~ 50 GeV in terms of A_{eff} and detection sensitivity, which limits the need to extend the energy bandpass to the highest energies where almost all analyses would be signal-limited. This in turn suggests that for future instruments, the balance between improving the PSF or the A_{eff} should be pushed in favor of the PSF relative to the LAT. For a practical figure of comparison when considering instrument designs it would make sense to try and obtaining the best possible PSF while keeping the on-axis A_{eff} with a factor of two of the LAT over the energy bandpass of the instrument.

Interestingly, improving the PSF requires decreasing the MCS, which will also increase the sensitivity to polarization.

Increasing the Low-Energy A_{eff} . The low-energy A_{eff} (i.e, below 100 MeV) of the LAT is limited primarily be three factors. 1) The falling cross section for pair-conversion. 2) The need to pass through 3-layer of high-density converter to leave enough hits to reconstruct a track. 3) The dearth of information about the event deposited in the detector, which makes background rejection much more difficult. Fortunately, these issues can be mitigated by including the measurement of Compton-scattering events in the instrument design and by reducing the MCS scattering in the tracking volume.

Discussion

Choosing the FOV and the Instrument Geometry. The large FOV of the LAT and the all-sky survey mode it allowed has enabled many breakthroughs and is well-suited to the highly variable nature of many γ -ray emitting sources. It is worth recalling that the FOV of the LAT is 2.5 sr as compared to the un-occulted sky in low Earth orbit of 8.4 sr or 12.6 sr for the whole sky. Thus, the maximum potential gain in the FOV is somewhere between a factor of 3.5 to 5, depending on the orbit. Although not huge, this could be combined with a factor of 2 to 3 increase in the average effective area to obtain a factor of 10 increase in the acceptance without hugely increasing the size of the instrument, an important limitation in space missions.

On the other hand, the best ways to improve the PSF are to decrease the density of the material in the tracker and to space the tracking element further apart. Given the space limitations, both of these could result in a FOV that is somewhat smaller than the LAT's. These considerations present two alternate instrument geometries as opposite extremes to consider.

The first, designed to have an excellent PSF and a limited FOV, would be tall and relatively narrow, and maximize the lever-arm in the direction of travel of the incoming γ rays. Such an instrument would be suited to an observing strategy of scanning the Galactic plane with occasional pointings and limited surveys of high-Galactic latitude sources and regions.

The second, designed to maximize the FOV while retaining a very good PSF, would be as compact as possible for a given surface area, i.e., cubic or spherical. In this geometry, one of the challenges is to avoid building an intrinsic directionality into the instrument, e.g., a design with a tracker above a calorimeter is only sensitive to γ rays going “down”, can not exceed a FOV 6.3 sr, and is unlikely to do better than about FOV 3 sr unless the tracker is extremely squat. So, in this case it is worth considering novel geometries, such as a calorimeter sandwiched between two trackers.

An interesting alternative is the possibility of a “monolithic” instrument, i.e., one with a single sub-system that measures both the direction and energy of the incoming γ rays. In practice, this likely would be done in one of three ways, each of which would present substantial design challenges. 1) Adding a magnet to measure the momenta of the charged particles in the tracking volume. 2) Building a particle tracker that is several radiation lengths thick. 3) Increasing the readout granularity of a hodoscopic calorimeter to extent that it does not limit the PSF.

Conclusion

Summary We have presented a series of summaries of information that may be useful in the design of future high-energy γ -ray telescopes. Specifically, we have summarized the instrument performance factors critical for scientific goals, the physical mechanisms influencing the detector design, and the most popular detector technologies. We have also laid out the key trade-offs that must be considered.

Almost all of this information is available in greater detail elsewhere. However, we hope that this contribution will prove useful by consolidating the material in a single source.